LC GC
asia pacific
solutions for separation scientists

February/March 2018
Volume 21 Number 1
www.chromatographyonline.com

With a Peak generator in your lab you can forget about your instrument gas supply and focus on your analysis. Your gas flow is our top priority, that's why we have Peak Service Engineers located in every continent, delivering **rapid response on-site technical support** wherever your lab may be. What's more, our unique **comprehensive product warranty** covers every single part of your generator, giving you complete **peace of mind**. That's what we call the **Peak brand promise**.

A Peak gas generator will bring to your lab:

Convenience
Gas delivered on-demand, no cylinders to change or supply stocks to maintain

Consistency
Consistent gas quality and supply, no impurities or running out of gas

Economy
Eliminate on-going costs of cylinders, manage lifetime running costs

Safety
No pressurised compressed gas cylinders in your lab

Sustainability
No repeated gas deliveries, energy efficient

On-site service
Comprehensive on-site warranty and service plans

Contact us today to discover more!

www.peakscientific.com

LC GC
asia pacific
solutions for separation scientists

February/March 2018
Volume 21 Number 1
www.chromatographyonline.com

The Evolution of UHPLC

The role of particles, pressure, and instrument contribution

LC TROUBLESHOOTING
A guide to assessing peak purity

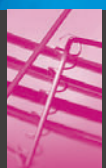

GC CONNECTIONS
The past and present of GC detection

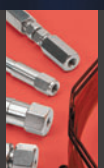

THE ESSENTIALS
SEC for biologics analysis

UBM

GILSON®

MAXIMISE YOUR CANNABIS PURIFICATION

Advantages of CPC Equipment:

- Isolate any type of cannabinoids or terpenes
- No product loss
- High purity achievable

www.gilson.com/cpc

Chromatography

MACHEREY-NAGEL

Manufacturer of premium chromatography media

Find what you are looking for!

- CHROMABOND® columns with classical and innovative SPE phases
- Original NUCLEOSIL®, professional NUCLEODUR® and highly efficient NUCLEOSHELL® HPLC columns
- Robust TLC glass plates, economical aluminum and polyester sheets

February/March | 2018

Volume 21 Number 1

COVER STORY

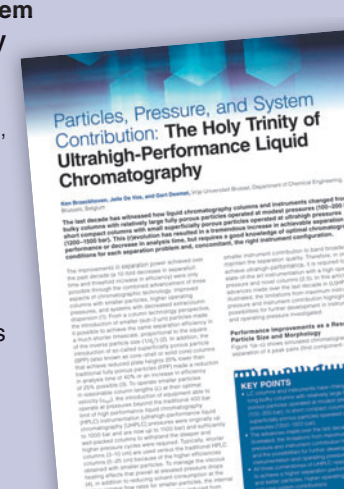

Columns

Departments

LC GC asia pacific
solutions for separation scientists

Editorial Policy:
All articles submitted to *LC•GC Asia Pacific* are subject to a peer-review process in association with the magazine's Editorial Advisory Board.

Cover:
Original materials:
De Space Studio/Shutterstock.com

The FFF - MALS Platform

Next Level Nano, Bio and Polymer Analysis

POSTNOVA

NEW
With SEC Option!

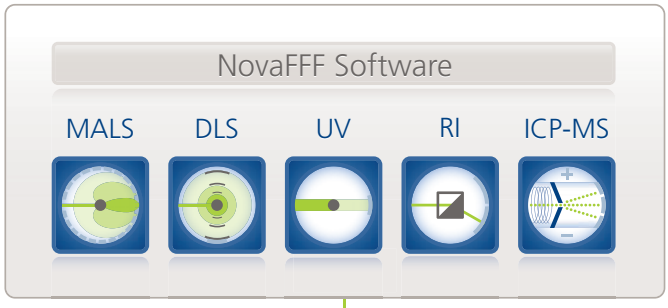

Contact us for more information: **www.postnova.com**

LC|GC asia pacific
solutions for separation scientists

Published by
UBM Americas

Vice President/Group Publisher
Mike Tessalone
michael.tessalone@ubm.com

Editorial Director
Laura Bush
laura.bush@ubm.com

Editor-in-Chief
Alasdair Matheson
alasdair.matheson@ubm.com

Managing Editor
Kate Mosford
kate.mosford@ubm.com

Associate Editor
Lewis Botcherby
lewis.botcherby@ubm.com

Sales Manager
Oliver Waters
oliver.waters@ubm.com

Sales Executive
Liz Mclean
liz.mclean@ubm.com

Senior Director, Digital Media
Michael Kushner
michael.kushner@ubm.com

Webcast Operations Manager
Kristen Moore
kristen.moore@ubm.com

Project Manager
Vania Oliveira
vania.oliveira@ubm.com

Digital Production Manager
Sabina Advani
sabina.advani@ubm.com

Managing Editor Special Projects
Kaylynn Chiarello-Ebner
kaylynn.chiarello.ebner@ubm.com

Art Director
Dan Ward
dward@hcl.com

Subscriber Customer Service
Visit (chromatographyonline.com) to request or change a subscription or call our customer service department on +001 218 740 6877

Hinderton Point,
Lloyd Drive,
Cheshire Oaks,
Cheshire,
CH65 9HQ, UK
Tel. +44 (0)151 353 3500
Fax +44 (0)151 353 3601

Subscibe on-line at www.chromatographyonline.com

SUBSCRIPTIONS: LC•GC Asia Pacific is free to qualified readers in Asia Pacific.
To apply for a free subscription, or to change your name or address, go to www.chromatographyonline.com, click on Subscribe, and follow the prompts.
To cancel your subscription or to order back issues, please email your request to magazines@superfill.com, putting LCGC Asia Pacific in the subject line.
Please quote your subscription number if you have it.

MANUSCRIPTS: For manuscript preparation guidelines, visit www.chromatographyonline.com or call the Editor, +44 (0)151 353 3500. All submissions will be handled with reasonable care, but the publisher assumes no responsibility for safety of artwork, photographs or manuscripts. Every precaution is taken to ensure accuracy, but the publisher cannot accept responsibility for the accuracy of information supplied herein or for any opinion expressed.

DIRECT MAIL LIST: Telephone: +44 (0)151 353 3500.
Reprints: Reprints of all articles in this issue and past issues of this publication are available (250 minimum). Contact Brian Kolb at Wright's Media, 2407 Timberloch Place, The Woodlands, TX 77380. Telephone: 877-652-5295 ext. 121. Email: bkolb@wrightsmedia.com.

The Publishers of LC•GC Asia Pacific would like to thank the members of the Editorial Advisory Board for their continuing support and expert advice. The high standards and editorial quality associated with LC•GC Asia Pacific are maintained largely through the tireless efforts of these individuals.

LCGC Asia Pacific provides troubleshooting information and application solutions on all aspects of separation science so that laboratory-based analytical chemists can enhance their practical knowledge to gain competitive advantage. Our scientific quality and commercial objectivity provide readers with the tools necessary to deal with real-world analysis issues, thereby increasing their efficiency, productivity and value to their employer.

THE 6 SHARPEST PERSPECTIVES

for focused science and technology solutions in life science

Millipore®
Proven Preparation, Separation, Filtration & Testing Products

SAFC®
Tailored Pharma & Biopharma Raw Material Solutions

BioReliance®
Expert Pharma & Biopharma Manufacturing & Testing Services

Sigma-Aldrich®
State-of-the-Art Lab & Production Materials

Milli-Q®
Pioneering Lab Water Solutions

Supelco®
Trusted Analytical Products

Merck has brought together the world's leading Life Science brands, so whatever your life science problem, you can benefit from our expert products and services.

To find out how the life science business of Merck can help you work, visit SigmaAldrich.com/advancinglifescience

#howwesolve

The life science business of Merck operates as MilliporeSigma in the U.S. and Canada.

MERCK

Particles, Pressure, and System Contribution: **The Holy Trinity of Ultrahigh-Performance Liquid Chromatography**

Ken Broeckhoven, Jelle De Vos, and Gert Desmet, Vrije Universiteit Brussel, Department of Chemical Engineering, Brussels, Belgium

The last decade has witnessed how liquid chromatography columns and instruments changed from long bulky columns with relatively large fully porous particles operated at modest pressures (100–200 bar), to short compact columns with small superficially porous particles operated at ultrahigh pressures (1200–1500 bar). This (r)evolution has resulted in a tremendous increase in achievable separation performance or decrease in analysis time, but requires a good knowledge of optimal chromatographic conditions for each separation problem and, concomitant, the right instrument configuration.

The improvements in separation power achieved over the past decade (a 10-fold decrease in separation time and threefold increase in efficiency) were only possible through the combined advancement of three aspects of chromatographic technology: improved columns with smaller particles, higher operating pressures, and systems with decreased extracolumn dispersion (1). From a column technology perspective, the introduction of smaller (sub-2-µm) particles made it possible to achieve the same separation efficiency in a much shorter timescale, proportional to the square of the inverse particle size ($1/d_p^2$) (2). In addition, the introduction of so-called superficially porous particle (SPP) (also known as core–shell or solid core) columns that achieve reduced plate heights 25% lower than traditional fully porous particles (FPP) made a reduction in analysis time of 40% or an increase in efficiency of 25% possible (3). To operate smaller particles in reasonable column lengths (L) at their optimal velocity (u_{opt}), the introduction of equipment able to operate at pressures beyond the traditional 400 bar limit of high performance liquid chromatography (HPLC) instrumentation (ultrahigh-performance liquid chromatography [UHPLC] pressures were originally up to 1000 bar and are now up to 1500 bar) and sufficiently well-packed columns to withstand the steeper and higher pressure cycles were required. Typically, shorter columns (3–10 cm) are used versus the traditional HPLC columns (5–25 cm) because of the higher efficiencies obtained with smaller particles. To manage the viscous heating effects that prevail at elevated pressure drops (4), in addition to reducing solvent consumption at the higher optimal flow rates for smaller particles, the internal diameter (i.d.) of the columns was also reduced from 4.6 mm for HPLC to 2.1 mm for UHPLC columns. This reduction in column volume requires a concomitant smaller instrument contribution to band broadening to maintain the separation quality. Therefore, in order to achieve ultrahigh-performance, it is required to have both state-of-the art instrumentation with a high operating pressure and novel columns (2,5). In this article, the advances made over the last decade in (U)HPLC are illustrated, the limitations from maximum instrument pressure and instrument contribution highlighted, and the possibilities for further development in instrumentation and operating pressure investigated.

Performance Improvements as a Result of Particle Size and Morphology

Figure 1(a–c) shows simulated chromatograms of the separation of 4 peak pairs (first component of each at

KEY POINTS

- LC columns and instruments have changed from long bulky columns with relatively large fully porous particles operated at modest pressures (100–200 bar), to short compact columns with small superficially porous particles operated at ultrahigh pressures (1200–1500 bar).
- The advances made over the last decade are illustrated, the limitations from maximum instrument pressure and instrument contribution highlighted, and the possibilities for further development in instrumentation and operating pressure investigated.
- All three cornerstones of UHPLC need to be improved to achieve a higher separation performance: smaller and better particles, higher operating pressures, and reduced system contributions.

Photo Credit: De Space Studio/Shutterstock.com

6 powerful propellers

to accelerate expert science and technology solutions in life science

Millipore®
Proven Preparation, Separation, Filtration & Testing Products

SAFC®
Tailored Pharma & Biopharma Raw Material Solutions

BioReliance®
Expert Pharma & Biopharma Manufacturing & Testing Services

Sigma-Aldrich®
State-of-the-Art Lab & Production Materials

Milli-Q®
Pioneering Lab Water Solutions

Supelco®
Trusted Analytical Products

Merck has brought together the world's leading Life Science brands, so whatever your life science problem, you can benefit from our expert products and services.

To find out how the life science business of Merck can help you work, visit SigmaAldrich.com/advancinglifescience

#howwesolve

The life science business of Merck operates as MilliporeSigma in the U.S. and Canada.

MERCK

Figure 1: Simulated chromatograms obtained for different column dimensions and particle sizes: (a) 4.6 × 250 mm, 5-µm FP; (b) and (e) 2.1 × 100 mm, 2-µm FP; (c) 3.0 × 100 mm; 2.7-µm SP, (d) 2.1 × 250 mm, 2-µm FP. Plate heights calculated according to $h = H/d_p = a+b/\nu_0+c\cdot\nu_0$ with $\nu_0 = u_0\cdot d_p/D_{mol}$ with $D_{mol} = 10^{-9}$ m^2/s and a = 0.75 or 0.5, b = 4, and c = 0.1 or 0.075 for FP and SP, respectively. All columns in (a–c) were assumed to be operated at u_{opt} yielding a $h_{min} = 2$ for the FP and 1.6 for the SP particles respectively; column (d) was operated at $0.76\cdot u_{opt}$ and (e) at $1.9\cdot u_{opt}$. Column pressure drops were calculated according to $\Delta P = L\eta u_{opt}/K_V$, with viscosity $\eta = 10^{-3}$ Pa·s, $\phi_{FP} = 800$, $\phi_{SP} = 650$, and $K_v = d_p^2/\phi$. Injection volume was scaled according to column cross-section.

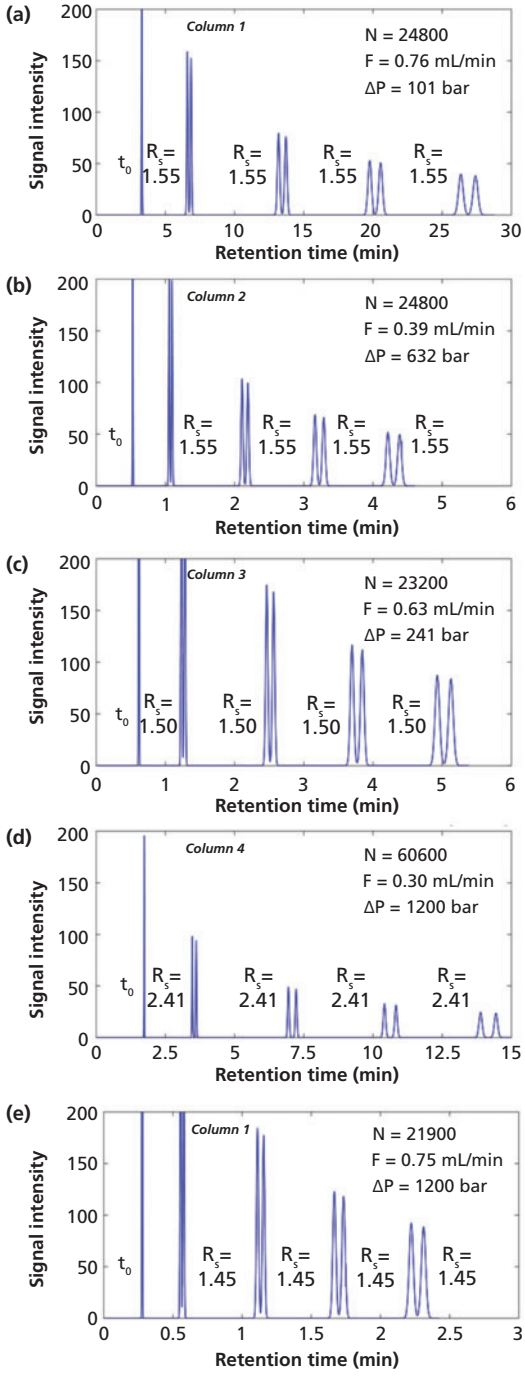

Figure 2: Comparison of the kinetic performance limits of HPLC (black) and UHPLC (red) instrumentation and columns for different particle sizes and column morphologies (FP = full symbols, SP = open symbols). Pressure limit: HPLC = 400 bar, UHPLC = 1500 or 1200 bar for 1.5-µm (SP) /2-µm (FP) and 2.7-µm (SP) particles, respectively. Retention factor $k = 9$, hence $t_R = 10\cdot t_0$. Other parameters same as Figure 1.

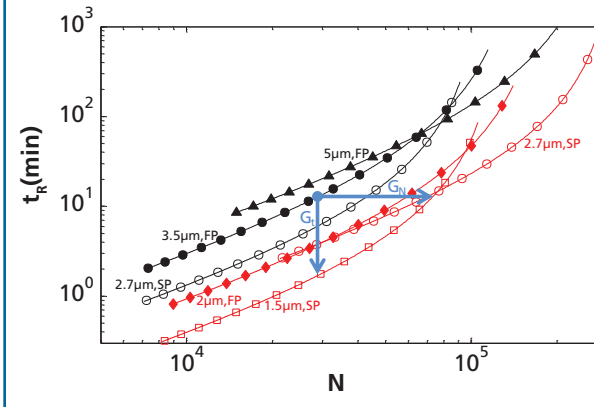

k = 1, 3, 5, and 7 and selectivities of 1.080, 1.053, 1.048, and 1.046, respectively to obtain the same resolution (R_s). Column 1 (Figure 1[a]) has the typical dimensions of routinely used columns on HPLC instrumentation, that is, 25-cm long with a 4.6 mm i.d. and packed with 5-µm FPPs (see Table 1 for an overview of the properties of the different columns). Column 2 (Figure 1[b]) represents its UHPLC equivalent (same plate count) of 10-cm long, but packed with 2-µm FPPs, each operated at its optimum velocity and assuming a reduced plate height $h = H/d_p = 2$. It becomes immediately clear that the same separation efficiency and resolution is achieved in both separations, but 6.25 times faster on Column 2. The latter separation, however, also requires the same increase in operating pressure, exceeding that of standard HPLC instrumentation (400 bar). The corresponding flow rate for Column 2 was calculated assuming a narrow internal diameter (2.1 mm) column typically used in UHPLC. As mentioned earlier, besides a reduction in solvent consumption, these narrower internal diameter columns are required to compensate for the increased viscous heating effects that occur at elevated pressure drops required to operate them at or above their optimal velocity. A good compromise between gain in analysis time and increase in pressure drop can be obtained when switching from a FPP column to a column packed with 2.7-µm SPPs (Figure 1[c], Column 3). These particles not only typically have minimum reduced plate heights closer to 1.5, but also, because of the lower porosity and lower flow resistance ϕ (15–20%) require lower pressure drops for similar velocities. As a result, with much larger particles (2.7 µm versus 2 µm) roughly the same efficiency (-6.5%) can be obtained for only a small increase in analysis time (+17%), as can be seen when comparing Figure 1(c) (Column 3) with Figure 1(b) (Column 2). The main advantage lies in the much lower operating pressure for the 2.7-µm particles (versus the

2 µm particles) required to run this column at its optimum flow rate (3). The required pressure is in fact only 2.4 times higher than for the 5-µm FP particles. For this reason a 3 mm i.d. was considered for Column 3 because the issue of viscous heating at these lower pressures is much less pronounced (3). Recently, it was demonstrated that FPPs with a narrow particle size distribution can reach minimum reduced plate heights of 1.7–1.9, that is, in between those of traditional fully porous (h = 2) and SPPs (h = 1.5) (6).

Gains in Analysis Time and Efficiency With Operating Pressure

Figure 1 shows how the same separation quality is achieved in a shorter time by changing particle type and size. However, it is also possible to keep the same analysis time (or have a smaller gain in analysis time), but increase the separation quality by using longer columns. Figure 1(d) shows the separation on a 25-cm long column with 2-µm FPPs (Column 4). If run at the optimal velocity, this would require an operating pressure above 1500 bar. To represent more realistic conditions, the flow rate was limited to that corresponding with a pressure limit of 1200 bar (which all UHPLC instruments can currently reach), resulting in a velocity slightly (-24%) below the optimal velocity. Nevertheless, the 2-µm particles can be operated at twice the velocity as the 5-µm particles (2.5 times faster in the absence of the pressure limitation), yielding a reduction in analysis time of a factor of two, a gain in efficiency of 2.4, and an increase in resolution of 1.6 (since $R_S \sim N^{0.5}$). An additional benefit of using small particles is that they can be operated at velocities above their optimum and only experience a small loss in performance because the C-term contribution to H is proportional to d_p^2. This is illustrated in Figure 1(e), where Column 2 is operated at almost twice (1.9×) its optimal velocity (limited to ΔP = 1200 bar). Whereas little or no efficiency and resolution is lost, the separation is performed almost twice as fact.

To combine the optimization of mobile phase velocity, column length, and particle size and at the same time take into account the pressure limitations of a system or column, the so-called kinetic plot methodology (7–11) provides a more concise way to compare the separation performance in (U)HPLC. By plotting the kinetic performance limits (KPL), that is, the shortest possible time to reach a certain performance, or, equivalently, the highest possible performance that can be reached for a given analysis time, the most optimal conditions for each chromatographic support (particle size and type) are compared (8,10). These limits are obtained by operating at the maximum pressure (400 bar for HPLC, 1200–1500 bar for UHPLC) and optimizing the column length. Such KPLs are plotted in Figure 2(a), which is an updated version (simplified) of figure 1 in reference 9 and figure 3 in reference 12. The figure provides an historic overview

Figure 3: (a–b): Experimental demonstration of the kinetic time-gain factor that can be achieved in isocratic mode for the separation of alkylphenones when going from (a) a system with three coupled columns packed with 2.6-µm particles operated at 486 bar to (b) an optimized system of two coupled columns packed with 1.5-µm particles operated at 1402 bar. A separation of wastewater pollutants by applying a linear gradient (ratio gradient time t_G over column void time t_0 as t_G/t_0 = 12, gradient range D_j = 0.75), while maintaining the same peak capacity, conducted on (c) two coupled columns packed with 1.5-µm core–shell particles operated at 495 bar and (d) one column packed with 1.5-µm core–shell particles operated at 1399 bar. Adapted with permission from reference 13.

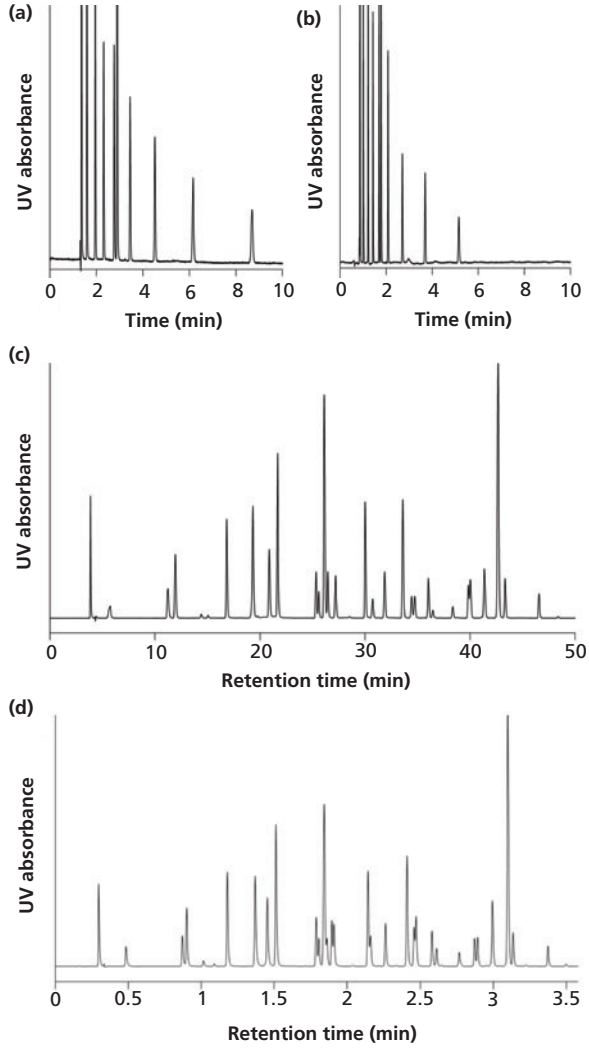

Figure 4: Similar conditions as Figure 1(a–d), but now assuming extracolumn volumetric dispersion contribution of 50 µL^2, typical for HPLC instruments, and assuming a total tubing length of 50 cm with an internal diameter of 170 µm for the calculation of the pressure.

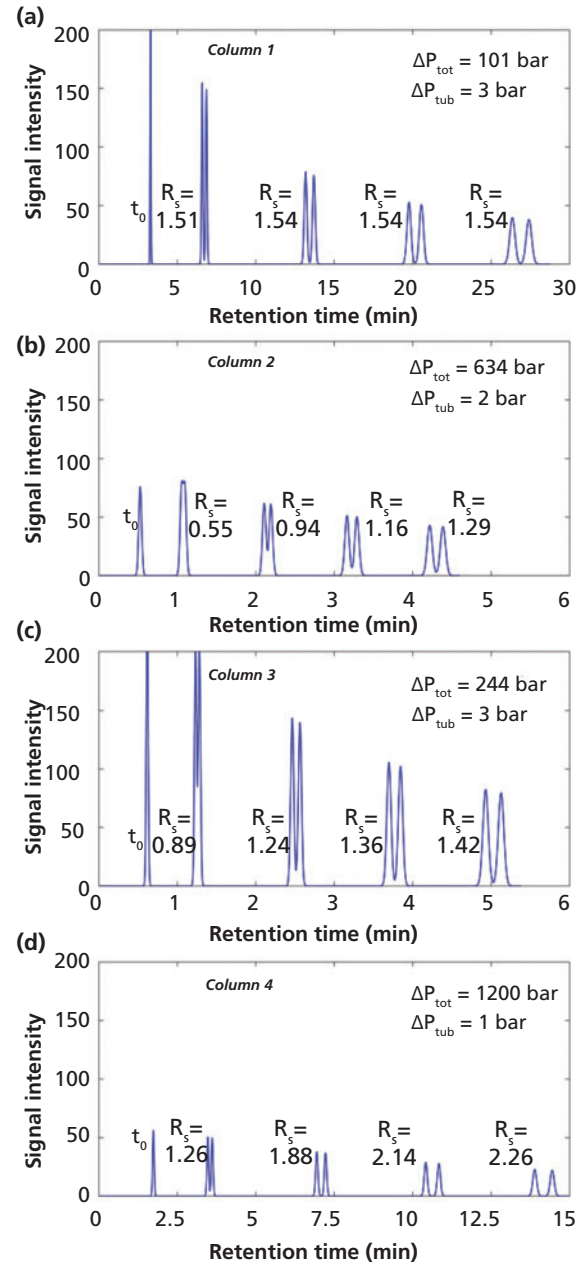

Table 1: Overview of the parameters of the different simulated columns (Figures 1, 4, and 5)

Column	Length (cm)	Diameter (mm)	Particle Size (µm)	Particle Type
1	25	4.6	5.0	Fully porous
2	10	2.1	2.0	Fully porous
3	10	3.0	2.7	Superficially porous
4	25	2.1	2.0	Fully porous

of the progress made from HPLC (black, 3.5–5-µm FPP, and 2.7-µm SPP) towards UHPLC particles and conditions (red, 2-µm FPP, 1.5- and 2.7-µm SPP) by plotting analysis time t_R (calculated as $t_R = t_0 \bullet (1 + k)$ with k = 9) versus efficiency N. The advantage of a higher operating pressure is clear because the red curves are located lower (faster analysis) and more to the right (higher efficiency) (8,9). In addition, the higher operating pressure favours the use of smaller particles.

For HPLC, the advantage of SPPs clearly stands out because they outperform 3.5-µm particles over the entire relevant range of efficiencies (the range where 3.5-µm particles have a better kinetic efficiency than 5-µm particles) (8). A similar conclusion can be drawn for the UHPLC separations, where the SPPs outperform their FPP counterparts, even though for the 2.7-µm particles a lower pressure limit (1200 bar) is assumed than for the 2-µm FPPs (where we took 1500 bar—currently the highest commercially available instrument pressure—as for the 1.5 µm SPPs). It can also be shown that the benefits of an increase in operating pressure and the use of more efficient superficially porous columns are additive. This methodology also allows kinetic gain factors that quantify the gain in analysis time (G_t) (for the same N) or efficiency (G_N) (for the same t) that can be reached by switching from one (old) operating pressure, particle type, and size to another (new) combination to be defined (1,9).

$$G_t = \frac{t_{old}}{t_{new}} = \frac{E_{old}}{E_{new}} \cdot \frac{\Delta P_{new}}{\Delta P_{old}}$$

$$G_N = \frac{N_{new}}{N_{old}} = \sqrt{\frac{E_{old}}{E_{new}} \cdot \frac{\Delta P_{new}}{\Delta P_{old}}} \qquad [1]$$

$$\text{with } E = \frac{H^2}{K_{v0}} = h^2 \cdot \varphi$$

In these expressions, E represents the separation impedance determined by the square of the plate height H (at the chosen flow rate) divided by the column permeability K_{v0} based on the velocity u_0 of an unretained compound ($K_{v0} = d_p^2/\phi$, with ϕ the flow resistance). For the arrows given in Figure 2 (N_{old} = 30000, $t_{R,old}$ = 13.6 min), both starting (ΔP_{old} = 400 bar) and ending (ΔP_{new} = 1500 bar) on a kinetic plot, the gains when switching from HPLC with 3.5-µm FPPs to UHPLC with 1.5-µm SPPs are G_t = 7.6 ($t_{R,new}$ = 1.8 min) and G_N = 2.48 (N_{new} = 74500). For these analysis times and conditions, the 3.5-µm FPP column at 400 bar for t_R = 30 min is operated at a velocity close to the optimum regime (h = 2.12; E = 3596). This is also the case for the 1.5 µm particles operated at 1500 bar such that t_R = 2.79 min (h = 1.66; E = 1791). For the 1.5 µm t_R = 13.6 min case, slightly larger particles would be better suited because the column is operated just below the optimal velocity, that is, in the B-term regime (h = 1.84; E = 2200).

Figure 3(a) and 3(b) represent results from an experimental investigation of these gain factors in isocratic mode (13). By switching from three coupled 10-cm columns (30 cm) packed with 2.6-µm core–shell particles operated at almost 500 bar (H_{old} = 5.46 µm, K_{v0} = 14.8 10^{-15} m^2, Figure 3[a]) to two coupled 10-cm columns (20 cm) with 1.5-µm core–shell particles operated at 1402 bar (H_{new} = 3.96 µm, K_{v0} = 3.8 10^{-15} m^2, Figure 3[b]), a nearly equivalent separation efficiency was measured (N_{old} = 54,900 versus N_{new} = 50,500, respectively), but a kinetic time gain factor of 1.6 was achieved. The gain in analysis time by a factor of 1.6 is slightly higher than the theoretically calculated value, which is only G_t = 1.4, but this theoretical value assumes

Figure 5: (a–d) Similar conditions as Figure 4(b–c), but now assuming a volumetric extracolumn dispersion contribution of 10 µL^2 (a–b) and 2 µL^2 (c–d), typical for an UHPLC and a fully optimized UHPLC instrument respectively, (e) 0.5 µL^2 volumetric extracolumn dispersion at u_{opt}/3.4 (ΔP_{max} = 1200 bar). Tubing length of 50 cm with an internal diameter of 75 µm (a–b), 50 µm (c–d), and 25 µm (e).

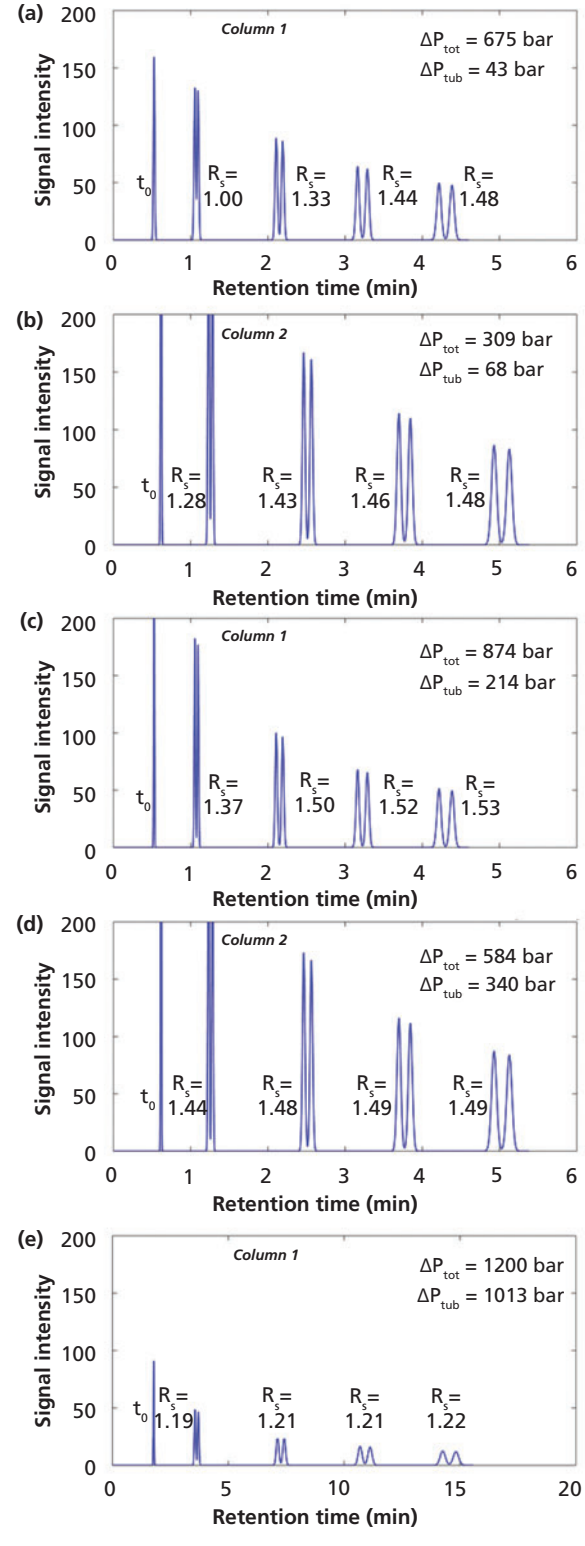

Figure 6: (a) Plot of plate number (N) versus retention factor (k) for a series of alkylphenones (aceto-, propio-, butyro-, benzo-, and valerophenone) showing the effect of the internal diameter of the post-column connection tubing in isocratic mode at a flow rate of 0.8 mL/min on an 2.1 × 50mm column packed with 1.3-µm superficially porous particles. (b) Overlay of a zoom-in on benzophenone eluting in gradient mode at a $k_{grad} = (t_R\text{-}t_0)/t_0$ of 4.5 and $k_{elution}$ of 1.8 at a flow rate of 0.6 mL/min using the same column. Adapted with permission from reference 20.

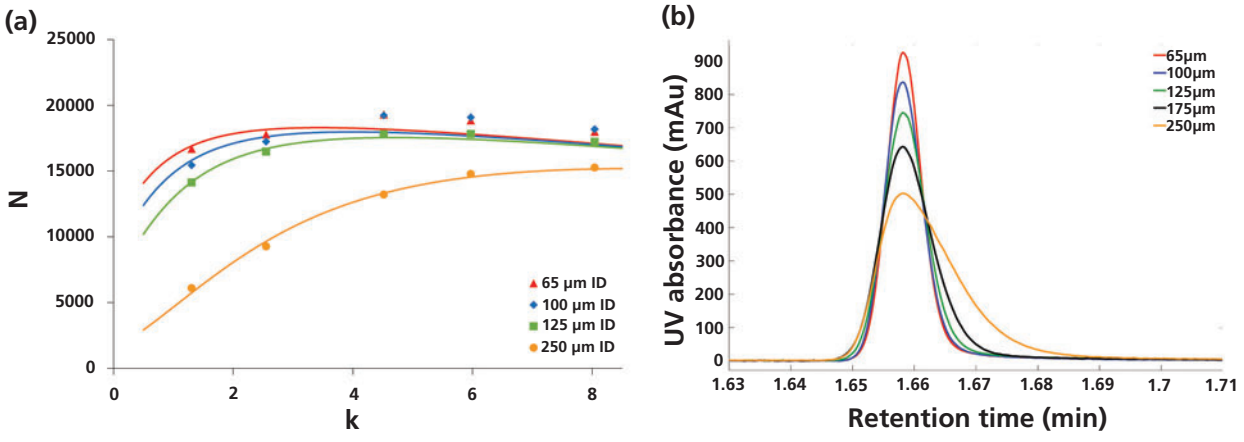

that exactly the same efficiency N is reached for both separations. However, as the separation efficiency in the improved ("new") system is around 10% lower than for the "old" system because of practical limitations (available column lengths), a larger gain in analysis time is found for slightly less efficiency. To obtain the same N, a slightly longer column (~10% larger, corresponding to a 22-cm column) should have been used at a slightly lower flow rate (also ~10% smaller), resulting in a time gain closer to 1.4 than the experimental value of 1.6. Figure 3(c) and 3(d) demonstrate the kinetic-time gain that can be achieved by optimizing a gradient separation of wastewater pollutants. A linear gradient from 20:80% (*v/v*) acetonitrile–water to 95:5% (*v/v*) acetonitrile–water was applied with $t_G/t_0 = 12$. By using 1.5-µm core–shell particles, and going from two coupled columns operated at 500 bar (Figure 3[c]) to one column operated at 1400 bar (Figure 3[d]), a kinetic time-gain factor of almost 13 was achieved. Although almost exactly the same peak capacity of around 190 was achieved (13), some differences in selectivity and resolution can be seen on the two chromatograms. These deviations are the result of pressure and temperature (viscous heating effects) gradients that induce changes in retention factor that can affect separation quality (4,14,15).

Requirements Regarding Instrumentation Contribution to Dispersion

For the sake of comparison, it was assumed that for the separations in Figure 1 the instrument did not contribute to the overall band broadening. However, it is obvious that the size of the injection plug (volume), diameter of the connection tubing, and volume of the preheater and detection cell all have an impact on the separation efficiency (16). Figure 4 therefore represents the same column performance ($N \approx 25000$) as considered in Figure 1, but assuming an additional system contribution to dispersion of 50 µL^2, which is a typical value for a standard HPLC instrument (5,17) and assuming connection tubing with an internal diameter of 170 µm and a total length of 50 cm to calculate the total system operating pressure. Whereas for Column 1 (the long wide-bore column packed with large 5-µm particles) little or no effect of extracolumn dispersion can be observed, the separation quality on the shorter narrow bore Column 2 with 2-µm particles is completely gone, showing a complete overlap for the early eluting pair and still a significant loss in resolution for late-eluting compounds. Since both columns are operated on the same system, Column 2 is much more affected because it has a much smaller volumetric dispersion as a result of the smaller column volume (1/12th) (18). For Column 3, packed with SPPs, the loss in performance from extracolumn dispersion is still significant, but smaller because a larger internal diameter (3 mm) can be used. The large internal diameter of the connection tubing ensures that little or no additional pressure is required at the represented flow rates. For the case of Column 4 (25-cm long with 2-µm particles), a significant loss in resolution is observed, but, as the longer and thus larger volume column is less affected by extracolumn dispersion and the superior performance already resulted in a higher resolution than necessary, the baseline separation ($R_S = 1.5$) is only compromised for the first eluting pair. Figure 4 illustrates how the switch to smaller particles or more efficient particle morphologies (SPPs) alone is not sufficient to obtain a better separation performance, but that the dispersion in the chromatographic system also needs to be considered (5).

Figures 5(a) and 5(b) show the obtained performance for Column 2 and Column 3 (the performance of

Column 1 was only negligibly affected by the system and is not shown), but now with the typical dispersion (17) for a UHPLC instrument—10 μL^2—and assuming this requires the same tubing length as in Figure 4 (50 cm) but now with an internal diameter of 75 µm. A significant improvement of the separation, especially for the early-eluting compounds, can be observed (18–21). Nevertheless, the early-eluting compounds are not yet baseline resolved. In addition, a significant increase in operating pressure from the narrower tubing is obtained. This increase is larger for Column 3 packed with SPPs because of the larger flow rate (see Figure 1). To get the full benefits from the narrow internal diameter columns, it is thus required to operate them on a fully optimized UHPLC system with reduced extracolumn dispersion. A number of groups have reduced the extracolumn dispersion to values as low as 2 μL^2 (20,21,22,23). This allowed them to obtain more than 90% of the intrinsic column efficiency for retention factors > 3. This is illustrated in Figures 5(c) and 5(d), which show little or no loss in separation resolution for all peaks except at $k = 1$. However, there is a steep increase in operating pressure as a result of the reduced internal diameter of the connection tubing. Once again, this is more pronounced for the 3-mm i.d. column (Column 3) where more than 60% of the total pressure drop is a result of the connecting tubing (versus around 30% for Column 2, with a 2.1 mm i.d.). In fact, for this case, the further decrease in extracolumn dispersion results in only a small gain in resolution but at a large cost in pressure drop. When a reduction in extracolumn volume results in such a cost in pressure drop that column length or flow rate has to be decreased, it will never be advantageous from a performance perspective. As an example, Figure 5(e) assumes connecting tubing of 25 µm i.d. and a system dispersion of 0.5 μL^2 for Column 2. The excessive pressure drop (at a fixed flow rate $\Delta P_{tub} \sim d_{tub}^4$) meant that the mobile phase velocity had to be decreased by a factor of 3.4 and therefore the column was operated far into the *B*-term regime. As can clearly be seen, this results in a significant increase in analysis time and a decrease in separation resolution. As an alternative (results not shown), one could opt for a 4.6 mm i.d. column packed with 2.7-µm SPPs, in which case even on the HPLC system with 50 μL^2 a resolution of 1.29 is found for the first peak pair, but, with the 170-µm tubing, only an operating pressure of 247 bar is required. The price to be paid is however a higher solvent consumption because the flow rate increases by a factor of around 2.4 and, although the pressure drop is limited, viscous heating related performance can become more pronounced if larger internal diameter columns are used.

Examples of System Contributions in Gradient and Isocratic Elution

Figure 6(a) and 6(b) illustrate how the optimization of extracolumn volumes can affect separation performance in both (a) isocratic and (b) gradient separations (20).

In this case, a small volume column (2.1 × 50 mm) packed with very small SPPs (1.3 µm) was run on a fully optimized chromatographic system (on-column focusing with POISE [24], 80 nL UV detector cell, minimized pre-column tubing) except for the short (14 cm) tubing connecting the column end with the detector cell. For this tubing, different internal diameters were chosen from 65 to 250 µm. For the isocratic case, the variation of the obtained separation efficiency (represented by the plate number *N*) versus retention factor is plotted. Even if only one part of the flow path—in this case the short 14-cm tubing from the column to the detector—is not optimized, a significant loss in performance already occurrs as for $k < 4$ a much lower efficiency than the expected $N = 20{,}000$ is found. As was illustrated in the previous simulated chromatograms, the first eluting compounds suffer most from the extracolumn band broadening (18,19,21). The slight downward trend in efficiency at higher retention factors results from the effect of retention factors on plate height and optimum velocity (20). In Figure 6(b), a zoom-in on one peak (benzophenone) in gradient elution mode is shown for the different tubing internal diameters. This compound elutes around an (apparent) gradient retention factor k_{grad} of 4.5. It can readily be seen that the wider tubing has a significant impact on the peak widths and heights. It is also clear that, contrary to what is often assumed, extracolumn band broadening can also have a significant impact in gradient mode because postcolumn dispersion is not minimized as a result of the typical on-column focusing at the start of a gradient run. For example, Spaggiari *et al.* demonstrated that when coupling UHPLC with MS, the interface tubing has to be minimized to have negligible impact on performance for *k* values greater than 7 for a standard system (25) and optimal MS settings need to be applied (18,25).

Conclusions

Faster or better separations can be obtained by switching to smaller particles and by using superficially porous particles. However, smaller particles require higher operating pressures. To avoid pressure drop limitations caused by viscous heating and to reduce solvent consumption, these small particles are packed in short columns with a narrower internal diameter. As a consequence, the performance of these small volume columns is strongly affected by the extracolumn dispersion in the chromatographic system. This article has shown that all three cornerstones of UHPLC need to be improved to achieve the expected higher separation performance: smaller and better particles, higher operating pressures, and reduced system contributions.

References

(1) J. De Vos, K. Broeckhoven, and S. Eeltink, *Anal. Chem.* **88**, 262–278 (2016).
(2) S. Fekete, E. Oláh, and J. Fekete, *J. Chromatogr. A* **1228**, 57–71 (2012).
(3) J. Ruta, D. Zurlino, C. Grivel, S. Heinisch, J.-L. Veuthey, and D. Guillarme, *J. Chromatogr. A* **1228**, 221–231 (2012).
(4) D. V. McCalley, *TrAC Trends Anal. Chem.* **63**, 31–43 (2014).
(5) K.J. Fountain, U.D. Neue, E.S. Grumbach, and D.M. Diehl, *J. Chromatogr. A* **1216**, 5979–5988 (2009).
(6) O.H. Ismail, M. Catani, L. Pasti, A. Cavazzini, A. Ciogli, C. Villani, D. Kotoni, F. Gasparrini, and D.S. Bell, *J. Chromatogr. A* **1454**, 86–92 (2016).
(7) K. Broeckhoven, D. Cabooter, and G. Desmet, *LCGC Europe* **24**, 396–404 (2011).
(8) K. Broeckhoven, D. Cabooter, S. Eeltink, and G. Desmet, *J. Chromatogr. A* **1228**, 20–30 (2012).
(9) K. Broeckhoven and G. Desmet, *TrAC Trends Anal. Chem.* **63**, 65–75 (2014).
(10) P.W. Carr, X. Wang, and D.R. Stoll, *Anal. Chem.* **81**, 5342–5353 (2009).
(11) G. Desmet, D. Cabooter, and K. Broeckhoven, *Anal. Chem.* **87**, 8593–8602 (2015).
(12) R.E. Majors, *LCGC Europe* **28**, 658–665 (2015).
(13) J. De Vos, M. De Pra, G. Desmet, R. Swart, T. Edge, F. Steiner, and S. Eeltink, *J. Chromatogr. A* **1409**, 138–145 (2015).
(14) G. Vanhoenacker, F. David, B. Blatz, E. Naegele, and P. Sandra, "Increasing Productivity in the Analysis of Impurities in Metoclopramide Hydro-chloride Formulations Using the Agilent 1290 Infinity LC System", Application note, (2009) http://cp.chem.agilent.com/Library/applications/5990-3981EN.pdf.
(15) K. Broeckhoven, J. Billen, M. Verstraeten, K. Choikhet, M. Dittmann, G. Rozing, and G. Desmet, *J. Chromatogr. A* **1217**, 2022–2031 (2010).
(16) J.P. Grinias, B. Bunner, M. Gilar, and J.W. Jorgenson, *Chromatography* **2**, 669–690 (2015).
(17) S. Fekete and J. Fekete, *J. Chromatogr. A* **1218**, 5286–5291 (2011).
(18) S. Buckenmaier, C.A. Miller, T. van de Goor, and M.M. Dittmann, *J. Chromatogr. A* **1377**, 64–74 (2015).
(19) N. Lambert, S. Miyazaki, M. Ohira, N. Tanaka, and A. Felinger, *J. Chromatogr. A* **1473**, 99–108 (2016).
(20) K. Vanderlinden, K. Broeckhoven, Y. Vanderheyden, and G. Desmet, *J. Chromatogr. A*, **1442**, 73–82 (2016).
(21) F. Gritti, T. McDonald, and M. Gilar, *J. Chromatgr. A* **1420**, 54–65 (2015).
(22) K.J. Fountain and P.C. Iraneta, in *UHPLC in Life Sciences, No. 16,* D. Guillarme and J.-L. Veuthey, Eds., (RSC Chromatography monographs, Cambridge, UK, 2012), pp. 29–66.
(23) F. Gritti, T. McDonald, and M. Gilar, *J. Chromatogr. A* **1420**, 54–65 (2015).
(24) A.C. Sanchez, J.A. Anspach, and T. Farkas, *J. Chromatogr. A* **1228**, 338–348 (2012).
(25) D. Spaggiari, S. Fekete, P.J. Eugster, J.L. Veuthey, L. Geiser, S. Rudaz, and D. Guillarme, *J. Chromatogr. A* **1310**, 45–55 (2013).

Ken Broeckhoven is an associate professor in the Department of Chemical Engineering at the Vrije Universiteit Brussel, Brussels, Belgium. His research focuses on the development of novel ultrahigh-pressure liquid chromatography instrumentation, fundamental aspects of supercritical fluid chromatography (SFC), investigation of the parameters affecting column performance, and the modelling of flow effects in chromatographic systems.

Jelle De Vos is a postdoctoral researcher at the Department of Chemical Engineering at the Vrije Universiteit Brussel. He is currently developing novel multilayered rotor technology to advance multidimensional separations and establishing microfluidic chip technology for three-dimensional spatial liquid chromatography.

Gert Desmet is a full professor in biochemical and chemical engineering at the Vrije Universiteit Brussel. His research focuses on the miniaturization of separation methods and on the investigation of flow and mass transfer effects in chromatographic systems. He is the first or senior author of over 250 peer-reviewed papers and 10 patent applications.

Messe München
Connecting Global Competence

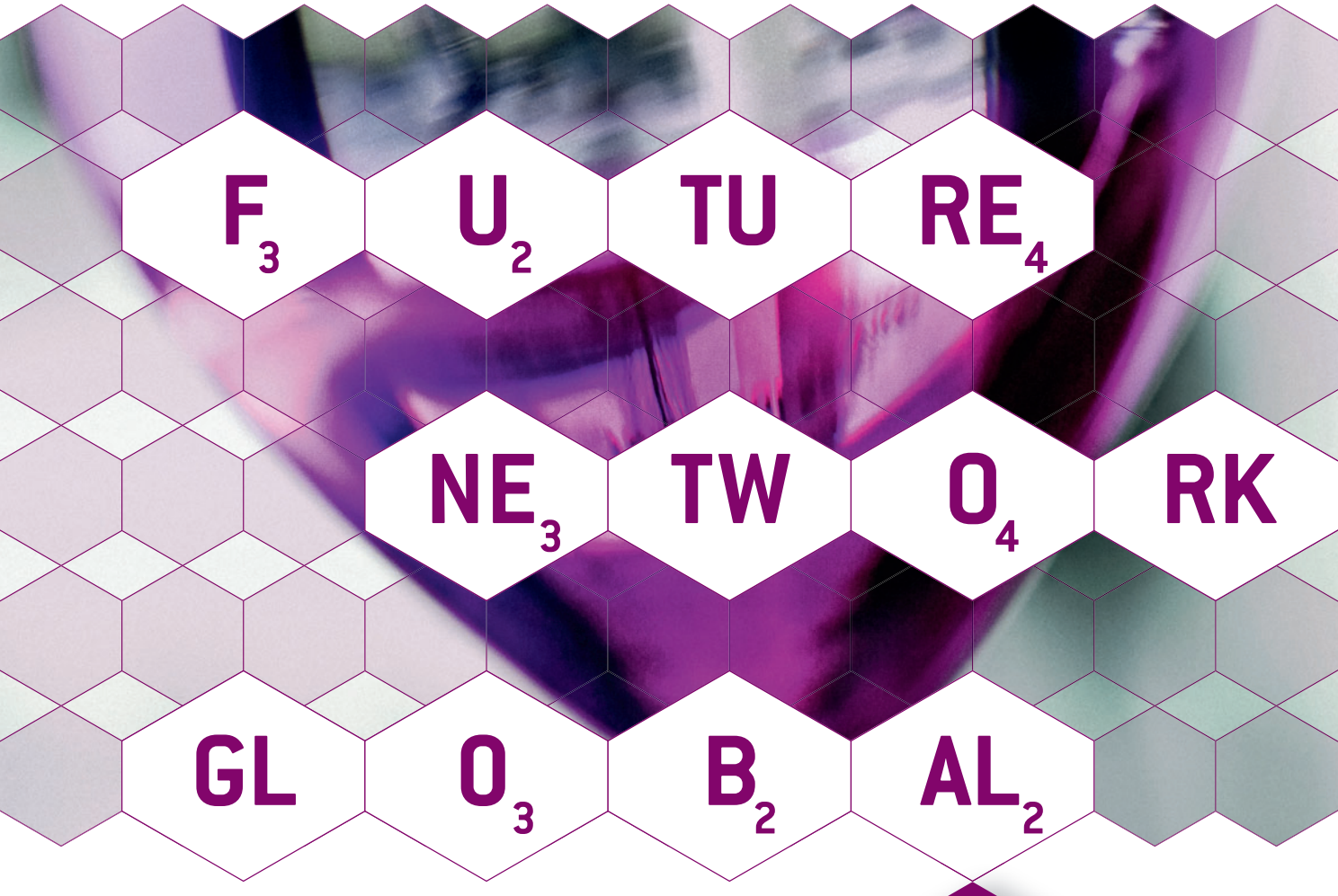

Highlights in 2018: Live Labs and Digital Transformation

The World's No. 1

The largest laboratory trade fair in the world features the entire range of products and solutions for industry and research laboratories.

The first-rate scientific analytica conference, world premieres, the latest product developments, unique Live Labs, special shows, forums and Focus Days await you!

April 10–13, 2018 I analytica exhibition
April 10–12, 2018 I analytica *conference*

26th International Trade Fair for Laboratory Technology, Analysis, Biotechnology and analytica conference
www.analytica.de

analytica

Peak Purity in Liquid Chromatography, Part 1: Basic Concepts, Commercial Software, and Limitations

Sarah C. Rutan[1], C.J. Venkatramani[2], and Dwight R. Stoll[3], [1]Virginia Commonwealth University (VCU), Richmond, Virginia, USA, [2]Genentech USA, San Francisco, California, USA, [3]LC Troubleshooting Editor

Is that peak "pure"? How do I know if there might be something hiding under there?

If we approach our data with a sceptical mindset, as chromatographers we know that there is always the possibility that a peak in a chromatogram that we perceive as a "pure peak" (that is, only one chemical component is eluted at that time) is actually composed of multiple coeluted components. From the point of view of quantitative analyses—answering the question "how much is there?"—this possibility is always a concern because assuming that a peak is pure when in fact it is not will lead to inaccurate quantitative determinations for the compound of interest. From the point of view of qualitative analyses—answering the question "what is it?"—it is a concern too, because if we think we have identified 10 components when in fact 11 components are present, we will have missed one, and that could have significant consequences (for example, impacts on health or profits). Given the importance of this issue, which we commonly refer to as "peak purity", an immense amount of research has been dedicated to the development of concepts and tools that can increase our confidence that we know what we are looking at in our chromatograms. However, 50+ years after the introduction of what we now call high performance liquid chromatography (HPLC), we arguably still do not have a one-size-fits-all solution to this problem. In this instalment of "LC Troubleshooting", we are tackling the peak purity topic in part 1 of a multi-part series where we will explore some of the concepts behind peak purity assessments, describe some tools that are used in commercially available software for these assessments, and highlight some of the limitations of these tools using real-world examples. For this purpose, I have enlisted two experts in data analysis and pharmaceutical analysis to work with me in addressing these issues. In subsequent instalments, we will expand our discussion of the peak purity topic to include advanced data analysis strategies that can be used in cases where simpler tools are inadequate, as well as the potential for two-dimensional liquid chromatography (2D-LC) to provide robust answers to questions about peak purity.

Dwight Stoll

Peak Purity: An Introduction

Of all of the application areas where the concept of peak purity is relevant, it has received the most concentrated attention in the pharmaceutical industry, and thus much of our discussion in this instalment is set in this context. Ensuring drug product quality and patient safety is the primary objective of the pharmaceutical industry and regulatory agencies around the world. Regulators expect that the pharmaceutical industry complies with the International Conference on Harmonization of Technical Requirements for Registration of Pharmaceuticals for Human Use (ICH) guidelines (*ICH Q3A – Q3D*) (1–4) on impurities in new drug substances and drug products, including residual solvents and elemental impurities. Significant effort on the part of both companies and regulators is dedicated to the delivery of safe and efficacious medications of desired quality and strength.

Various analytical tests that include methods to assess attributes ranging from appearance, identity including form, assay (weight or weight against a standard), impurities (organic and inorganic, including residual solvents), water content, and particle size analysis are performed on active pharmaceutical ingredients (APIs). Similarly, oral drug products (that is, the API plus excipients) are tested for appearance, identity, assay (weight or weight against a standard) and impurities, uniformity of dosage units, dissolution, microbial content, and water content. Among these tests, those for determinations of assay and impurities, including chiral impurities if applicable, are the most critical because they have the most potential to impact the safety and efficacy of the drug product.

Developing a specific, so-called "stability indicating method" to determine the drug substance and drug product content (weight or weight assay), quantitate impurities, and determine potential degradation products is extremely important because it provides evidence that the method is adequate to monitor the quality of the material during its shelf time. Developing this type of method usually starts with screening columns of different selectivity, using mobile phases at different pH values, and the analyses of samples of the drug product stressed by different means

(for example, acid, base, peroxide, light, and heat). Stressed samples are used upfront to assess the adequacy of the method to support long-term stability studies of drug products justifying their shelf life (or expiry). In addition, it can help to identify the likely degradation products and hence the degradation pathways. Increasingly, it is expected that method optimization software tools are used to ensure that methods are robust from the start—this is the spirit of the so-called quality-by-design (QbD) approach to method development (5). Typically, in these methods diode-array detection (DAD) or mass spectrometry (MS) is used to detect compounds as they are eluted from the column. To the extent that the spectrum (ultraviolet [UV] or mass) of a particular compound is characteristic of that compound, examination of the evolution of the spectrum across a peak provides a means to assess peak purity. However, impurities and degradation products eluted in the proximity of the main component are usually structurally similar. This, in turn, means that their DAD spectra are often highly similar, and great care is required in the interpretation of spectral purity assessments and consideration of complementary data that support the peak purity assessment (for example, elution patterns observed with complementary column selectivities, and MS data).

The presence of high potency impurities or inactive impurities in the dosage form can impact the biological activity of drug products. There are several well-known examples from the history of drug development that illustrate the importance of detecting coelutions. (*S*)-(+)-naproxen is effective in the treatment of arthritis, whereas its enantiomer causes liver poisoning. Similarly (*S,S*)-(+)-ethmbutol is effective in the treatment of tuberculosis, whereas its enantiomer causes blindness (6). Finally, *R*-thalidomide was known to be effective in the treatment of morning sickness; however, the enantiomer is a teratogen (7). Thus, accurate assessment of peak purity is critical to the assurance of the safety and efficacy of drug products.

Principles of Peak Purity Assessment Using DAD

As a chromatographer, the question most often asked when it comes to peak purity is: Is this chromatographic peak comprised of a single chemical compound? Unfortunately, there is no definitive answer for this question using the conventional peak purity methods that are available in commercial software. Rather, these software tools provide an answer to the question: Is this chromatographic peak composed of compounds having a single spectroscopic signature? This concept, typically referred to as *spectral peak purity*, can be addressed to varying degrees by most commercially available data systems for LC.

Theoretical Basis of Spectral Peak Purity Assessment:

The concept of spectral peak purity, as embodied in most chromatographic data systems, is based on viewing a spectrum as a vector in *n*-dimensional space, where *n* is the number of data points in the spectrum (8). To more easily visualize this concept, let us take an example of a spectrum measured at just three wavelengths, λ_1, λ_2, and λ_3, as shown in Figure 1(a). We can plot this spectrum as a vector in three-dimensional (3D) space as shown in Figure 1(b), where the vector terminates at a point with coordinates that are the absorbance values for the three wavelengths. Then, given a second spectrum, shown in red in Figure 1(c), we are interested in a way to quantify the similarity of the two spectra. A convenient means of assessing

Figure 1: (a) Depiction of a three-point spectrum; (b) representation of this spectrum as a vector in 3D space; (c) depiction of two, similar three-point spectra; (d) representation of these two spectra as vectors in 3D space, with the angle between the vectors representing the spectral similarity.

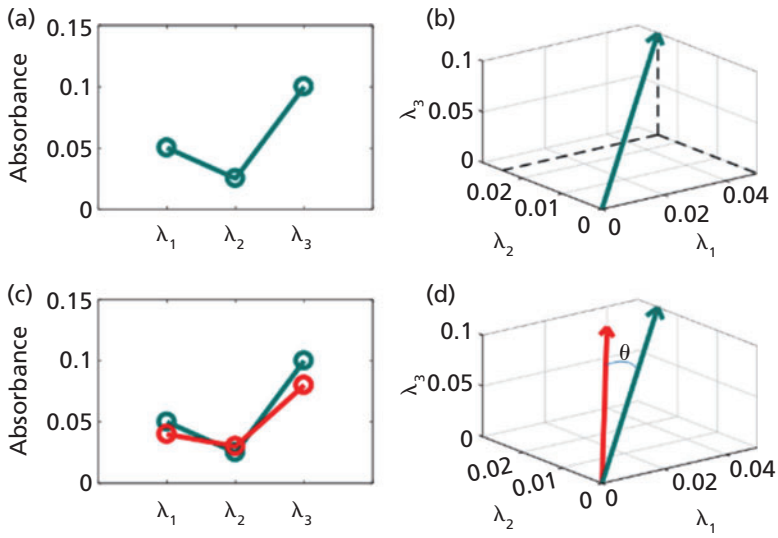

spectral similarity is to determine the angle between the two vectors that represents the spectra in *n*-dimensional space, as shown in Figure 1(d). If the angle Θ between the two vectors is zero, the shapes of the two spectra are identical (even if the overall intensities of the two spectra are different). If we denote the blue spectrum (vector) as spectrum a and the red spectrum (vector) as spectrum b, the spectral similarity can be calculated as the cosine of the angle Θ as follows:

$$\cos\theta = \frac{\mathbf{a}\cdot\mathbf{b}}{\|\mathbf{a}\|\,\|\mathbf{b}\|} = \frac{\Sigma a_i b_i}{\sqrt{\Sigma a_i^2}\,\sqrt{\Sigma b_i^2}} \quad [1]$$

where the bold face, lowercase letters denote vectors, or a list of the coordinates for the vector (three values in the present illustration; *n* values for the general *n*-dimensional case). The numerator represents the dot product of the two vectors, and the || || notation represents the vector norm, or in more conventional terms, the length of the given vector. Dividing by the length of the vectors results in a value for the spectral similarity that is independent of the amplitude of the signal and only dependent on the shape of the spectrum, as mentioned above.

An alternate means of determining the spectral similarity used by some chromatographic data systems involves the correlation coefficient between the two spectra, which is calculated as follows:

$$r = \frac{\Sigma(a_i-\bar{a})(b_i-\bar{b})}{\sqrt{\Sigma(a_i-\bar{a})^2\,\Sigma(b_i-\bar{b})^2}} \quad [2]$$

where the a_i and b_i values indicate the absorbance values at the *i*th wavelength. As long as the vectors are mean-centred prior to applying equation 1, it turns out that

$$r = \cos\theta \quad [3]$$

so that the two measures of similarity are equivalent.

Illustration of Spectral Similarity Determination Using Real Spectra: We next turn to a comparison of two similar, but not identical spectra to see how this concept of spectral similarity applies in practice. Figure 2 shows the spectra of two isomeric compounds, angelicin (blue) and psoralen (red). Applying mean centring, the cosine of the angle between them (and equivalently the correlation coefficient) is 0.980, and the angle (sometimes called the *spectral contrast angle*) is 11.4°. Without mean centring, the cosine of the angle is 0.988 and the corresponding angle is 8.97°. From inspection, it can be seen that these spectra, while similar, are not identical.

We now explore how to determine whether or not a particular chromatographic peak is pure using this metric. Figure 3(a) shows a chromatographic peak for which we would like to know the peak purity, and Figure 3(b) shows the contour plot for this peak, where the coloured contours indicate the absorbance at each time or wavelength point. The peak purity software provided by many chromatographic data system vendors points out the importance of baseline removal before peak purity analysis; this baseline is shown in Figure 3(a) as running from the peak start and stop limits (red hatch marks) from 9.9 to 12.7 min.

We then select the spectrum at the peak apex to serve as the reference spectrum (one option of several typically provided by the chromatographic data system vendor). It is often recommended to choose the apex from the "max" chromatogram (constructed using largest absorbance observed for each spectrum). Then, the similarity between this apex spectra and all the spectra across this peak (denoted by the index *j*) is evaluated, as shown in equation 4:

$$r = \cos\theta = \frac{\Sigma(a_{apex,i}-\bar{a}_{apex})(a_{j,i}-\bar{a}_j)}{\sqrt{\Sigma(a_{apex,i}-\bar{a}_{apex})^2\,\Sigma(a_{j,i}-\bar{a}_j)^2}} \quad [4]$$

The evolution of this similarity value across the peak is shown in Figure 3(c) by the green curve (shown as $1000r^2$; this is the match factor used by Agilent software; also note the inverted *y*-axis used in the Agilent software as well) (9,10). Although the correlation is quite high across the top of the peak, correlation values are lower on the leading edge of the peak, leading to the question of whether or not this peak is "spectrally pure". To more adequately address this question, we need to establish a threshold to determine whether or not this correlation is sufficiently high enough to conclude that this is a pure peak. It is at this point where the different vendors of chromatographic data systems apply slightly different approaches.

In the Agilent software, the threshold curve is calculated as shown in equation 5:

$$\text{Threshold}_j = 1000\left(1-0.5\left(Var_{noise}/Var_j + Var_{noise}/Var_{apex}\right)\right)^2 \quad [5]$$

where the variance of the noise (Var_{noise}) is calculated from a default or user

42nd International Symposium on Capillary Chromatography and 15th GC×GC Symposium

...with particular emphasis on all Comprehensive Separation Technologies and MS Hyphenation

13 - 18 May, 2018

Palazzo dei Congressi
Riva del Garda
Italy

The 42nd International Symposium on Capillary Chromatography (ISCC) and the 15th GC×GC Symposium is a "hyphenated" meeting which will be held again in wonderful Riva del Garda (Italy), from 13 to 18 May, 2018. Apart from the most recent advances in the fields of pressure and electrodriven microcolumn separations, and comprehensive 2D GC. This year particular emphasis will be directed to all Comprehensive Separation Technologies in combinations of Capillary Chromatography and 2D GC with various forms of MS... from unit-mass to high resolution, and from single to hybrid analyzers. Consequently, both the importance and complementary nature of chromatographic and MS processes will be given high consideration. Within the wider context of separation science, great space will be also given to the sample preparation process, in both oral and poster sessions. The ISCC/GC×GC scientific program will be a rich one, it being characterized by:

- invited contributions from leading scientists reporting the latest most exciting developments
- keynote lectures from promising young researchers
- very active poster sessions
- discussion sessions
- workshop seminars presenting the most recent novelties in scientific instrumentation
- a World-class GC×GC and LC×LC Short Courses

Researchers in all areas relevant to the subjects of the symposia are invited to submit abstracts. As is traditional for the Riva meetings, the majority of presentations will be in a poster format and the Scientific Committee will select contributions for oral presentations. As always, many awards will be assigned in both the ISCC and GC×GC events, recognizing excellence in both established and young scientists, in oral and poster presentations. Exhibitors and sponsors are a fundamental part of the meeting (without them...Riva wouldn't be Riva!) and are encouraged to participate by reserving booth space, becoming a sponsor and to promote the ISCC and GC×GC events.

Last, but not least, the traditional "Riva" social program will be entirely maintained, with one or two events each day: cocktails, the welcome reception, the concert, the wine and cheese evening, and of course, the disco night! Please keep visiting our web site (www.chromaleont.it/iscc) for new information as it becomes available.

Looking forward to meeting you in astonishing Riva del Garda!

Organized by

Chromaleont s.r.l.

The Forum of Microcolumn Separations

Figure 2: Spectra for angelicin (cyan) and psoralen (red). Spectral similarity expressed as $\Theta = 11.4°$; r = 0.980.

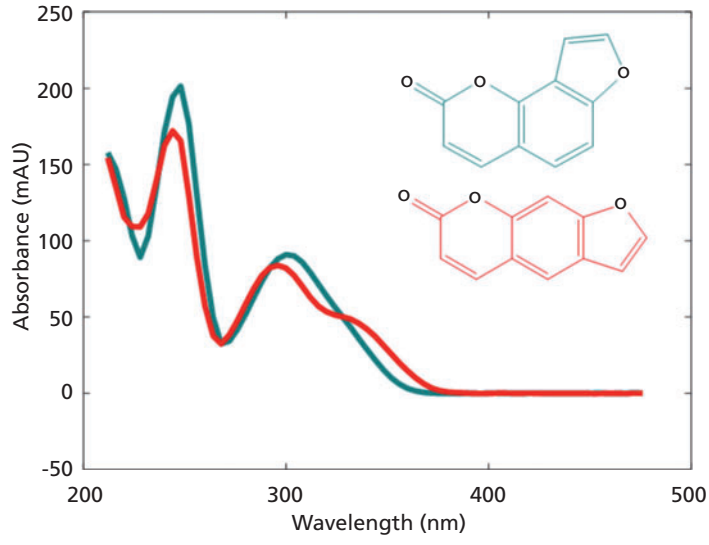

Figure 3: (a) Chromatographic peak with the reference spectra selected at the apex of the peak (green circle) and the noise spectra used for determination of the noise variance (Var_{noise}) (purple circle). (b) Representation of this chromatogram as a contour plot where the *y*-axis is the UV–vis absorbance spectrum and the *x*-axis is the chromatographic time axis. (c) Spectral similarity as compared to the apex (given by $1000r^2$) across the chromatographic peak profile (green) and the corresponding noise threshold (blue). Based on this plot we would conclude that the chromatographic peak is affected by a significant impurity before about 10.7 min.

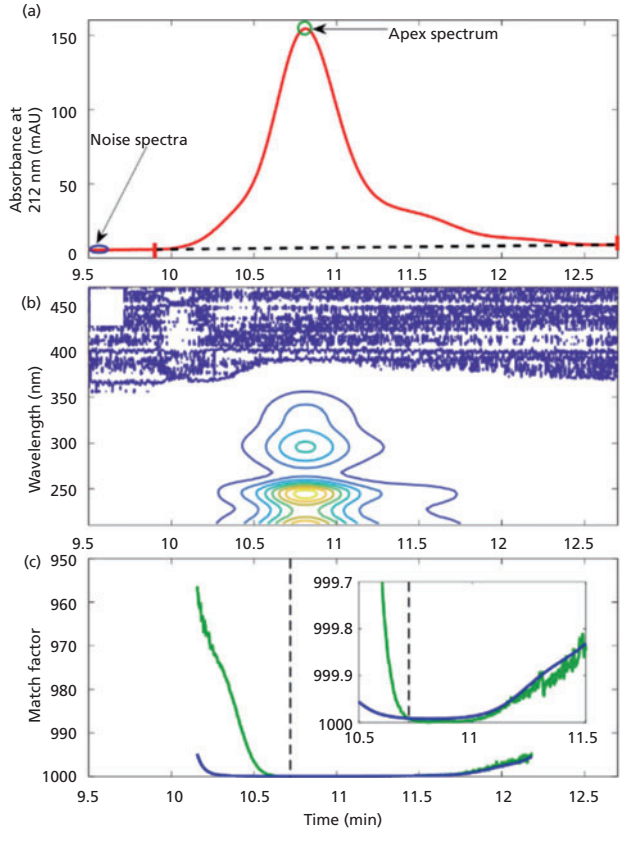

specified range of spectra where no analytes absorb, indicated by the purple circle in Figure 3(a). The Var_j is the variance of the *j*th spectrum and Var_{apex} is the variance of the apex spectrum (or another reference spectrum as specified by the user). This threshold curve is shown in purple in Figure 3(c). The inset figure shows an expanded view and indicates that this peak appears to be affected by an impurity at elution times earlier than about 10.7 min. In fact, this peak is composed of 50 ppm of psoralen (spectrum shown in red in Figure 2), with a retention time at 10.8 min, and 5 ppm of angelicin (spectrum shown in cyan in Figure 2), with a retention time at 10.4 min, which is the "impurity" detected by the software. In addition to providing a peak purity plot such as that shown in Figure 3(c), vendors often provide an overall peak purity measure and threshold for the entire peak. For example, Agilent determines the total number of spectra within the peak that are judged as impure by comparison of the match factor and threshold, and averages the match factor and thresholds for these spectra. For the example shown above, 1446 out of the 2430 spectra across the peak had match factors that were less than the corresponding threshold values, where the average match factor for these spectra was 992.8 and the average threshold was 999.0, again leading to the conclusion that this is an impure peak.

Other vendors of chromatographic data systems use variations on this general approach to quantify peak purity. For example, Shimadzu (11) uses the cosine of the similarity angle to quantify purity, and uses the following expression for the threshold

$$\text{Threshold}_j = \sqrt{\left(1-\frac{Var^2_{noise}}{\|a_{apex}\|^2}\right)\left(1-\frac{Var^2_{noise}}{\|a_j\|^2}\right)} - \frac{Var^2_{noise}}{\|a_{apex}\|\cdot\|a_j\|} \quad [6]$$

Meanwhile, Waters Empower software uses the similarity angle directly, and calculates a threshold based on both solvent and noise contributions (12). In using any of the chromatographic data system methods for assessing peak purity, it is critical to follow their guidance for baseline subtraction and noise estimation to get the most robust results for a spectral purity conclusion.

The concept of spectral similarity for assessment of peak purity using DAD is very useful in many situations, and it is attractive because of its low cost. A low spectral similarity value or match factor can provide an indication to the analyst that an impurity is present; however, high spectral similarities or match factors that indicate that the spectra across a peak are not significantly different may still occur for impure peaks for one or more of the following reasons:

- impurities are present at much lower concentrations (absorbances) than the main compound,
- the spectra for the main compound and the impurity are identical or very similar, and
- the impurity is coeluted with the main compound with a retention profile that has the same shape and retention time as the main compound (9).

Examples from Analyses of Real Pharmaceutical Materials

In the following case study we show examples from the analysis of a linker drug intermediate that highlights both the strengths and limitations of the spectral purity approach to assess peak purity. In this case, all peak purity calculations were carried out using Waters Empower 3 software. Synthesis and analysis of linker drug intermediates is extremely challenging because of their high reactivity, chemical instability, multistep synthetic routes, and relatively high molecular weight for a small molecule pharmaceutical (13). They are key component of antibody–drug conjugates (ADCs) used in oncology.

HPLC separations of three synthesis lots of linker drug intermediate are shown in Figure 4, with an expanded scale around the main linker drug peak. This plot shows lot-to-lot variability with multiple components eluted in the proximity of the main component. Developing an HPLC method to resolve these structurally similar compounds is challenging and requires peak purity assessment using DAD data along with MS detection, and screening of complementary column selectivities to minimize the likelihood of impurities coeluted with the main component.

Figure 4(a) shows the chromatographic profile of sample lot A with no noticeable peaks eluted in the trailing edge of the main component (retention time at 23.015 min) whereas sample lot B (Figure 4[b]) shows an impurity at a retention time of 23.354 min. In this example, only peaks in the trailing edge of the main component are integrated. The area percent of the impurity peak is 0.13% (Figure 4[b]). Sample lot C shows multiple components eluted in the trailing edge of the main component with a major impurity at 1.4% relative area (Figure 4[c]).

The results of peak purity analysis of sample lot A are shown in Figure 5. The purity angle of the main component (0.054) was less than the threshold (0.235), and the purity curve is below the threshold curve across the entire peak, indicating spectral homogeneity across the peak.

Figure 6(a) shows peak purity analysis of sample lot B. The main component peak (that is, the peak at 23.036 min) in this case passes spectral peak purity (false negative) even though a visibly noticeable impurity is present in the trailing edge of the peak as shown in Figures 4(b) and 6(b). The overall peak purity was determined to be 0.078 and the overall threshold was 0.235, indicating that the peak is spectrally pure. Possible explanations for this false negative include high spectral similarity between the main component and impurity peak, or the low level of the impurity relative to the main component

Figure 4: Chromatograms focused on the region of interest for sample lots A, B, and C. Peak purity assessment was limited to the peaks integrated in this window.

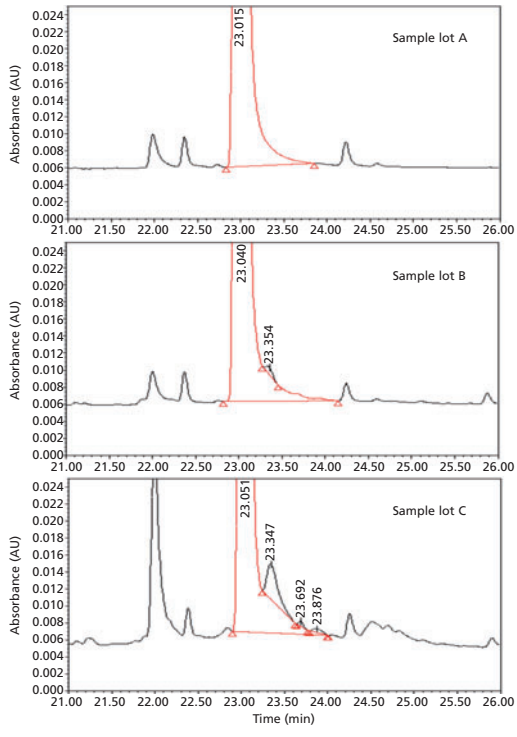

Figure 5: Peak purity analysis of sample lot A showing spectral purity across the integration limits of the peak: (a) Main component peak at 23.009 min; (b) expanded scale showing purity and threshold curves. The purity curve (green) is below the threshold curve (blue) across the peak (expanded plot).

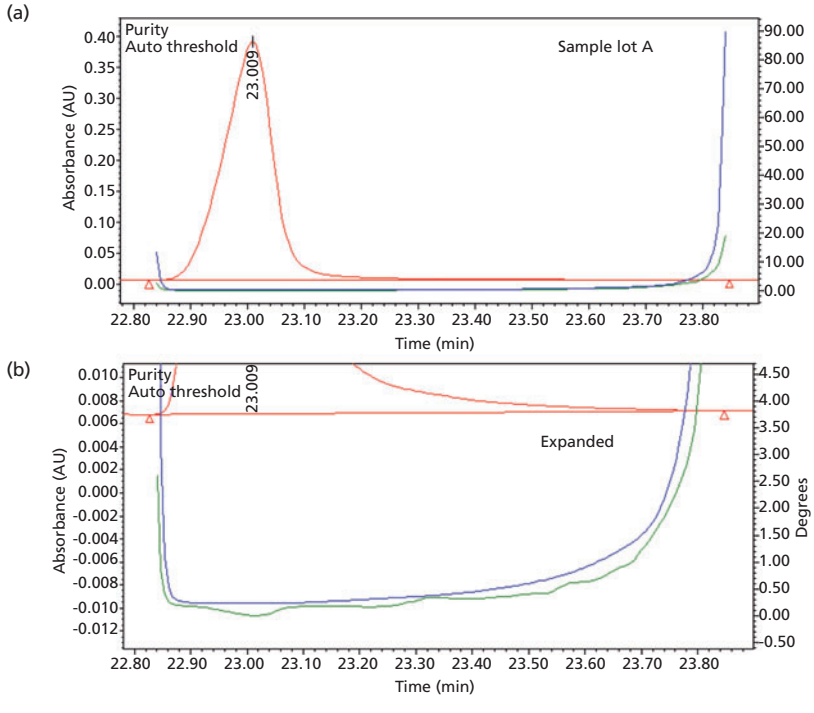

(~0.13%). The high degree of similarity in the normalized UV spectra of the main component and impurity peak (inset in Figure 6[a]) suggests that spectral similarity is likely to be the cause of the false negative. However, a closer examination of the purity and threshold curves as shown in Figure 6(b) indicates that impurities may be present throughout the tail of the peak. This evidence, along with the clear presence of the small peak in the tail, would allow the analyst to conclude that the peak is spectrally impure, despite the overall purity test indicating that the peak is pure.

Additionally, the impurity peak shown in Figure 6(b) (that is, the peak at about 23.35 min in Figure 4[b]) fails spectral purity at the leading edge of the peak, with a purity angle of 0.436 and a threshold of 0.272 (Figure 6[c]). This failure is probably because of the impact of the main component on the leading edge of the impurity peak or the presence of other impurities. It is clear in this example that a chromatographer would conclude an impurity is present, because of the chromatographic evidence and the peak purity plot, despite the conclusion of the spectral peak purity test. Further insights may be gained by inspection of the chromatogram for sample lot C shown in Figure 4(c). Here, several impurity peaks are evident in the tail of the main peak, and it is probably the presence of all these impurities (albeit at lower concentration levels) that led to the observed discrepancy between the threshold and purity curves for sample lot B, Figure 5(b). And interestingly, the purity and threshold curves are very close together for sample lot A at 23.35 min (Figure 5[b]), indicating that this impurity is probably also present in this lot, although at a lower concentration, such that both chromatographic and spectroscopic evidence lead to the conclusion that this is a pure peak. The important implication is that if this impurity peak was not as well resolved as in the present case, but was eluted completely underneath the main peak, there would be no chromatographic or spectroscopic evidence that an impurity is present, even for sample lots B and C.

Concluding Thoughts

This discussion of the principles of peak purity assessments using diode-array spectral data highlights both the capabilities and limitations of this type of

Focusing on Cutting-edge Technology & Products
in Pharmaceutical Lab Equipment

LAB WORLD CHINA
Laboratory, Analytical & Biotech Equipment

LABWorld China 2018

20-22 June 2018, SNIEC, Shanghai, China

40,000+ **Pharma Buyers**

15,000+ **R&D Professionals**

Led by Top Brands

BRAND, Malvern, TEGENT, Metrohm, Julabo, interscience, SYMPATEC, IDEX, IKA, sartorius, CORNING, ThermoFisher SCIENTIFIC, DKSH, LAUDA, AkzoNobel, Anton Paar, Cole-Parmer

Hot Events of 2018

- 2018 Drug Safety and Quality Management Forum
- InnoLAB Salon
  I. Chromatography II.Particle Size Analyzer
  III.Intelligence Laboratory
- Hot topic discussion on Pharm Lab and Supply Chain
- 5th China BioPh Outlook Summit

REGISTER NOW

Scan the QR code to get your free pass!

Co-located with:

CPhI china | P-mec

+86 10 58036295 / +86 21 33392256
Anthea.Ju@ubmsinoexpo.com

www.labworld-china.com

UBM

Figure 6: Peak purity analysis of sample lot B shows spectral purity across the peak irrespective of a peak eluted in the trailing edges of the peak: (a) Main component peak at 23.036 min; (b) expanded view showing the details of the purity and threshold curves for the main component; (c) expanded view showing the details of the purity and threshold curves for the impurity at 23.350 min.

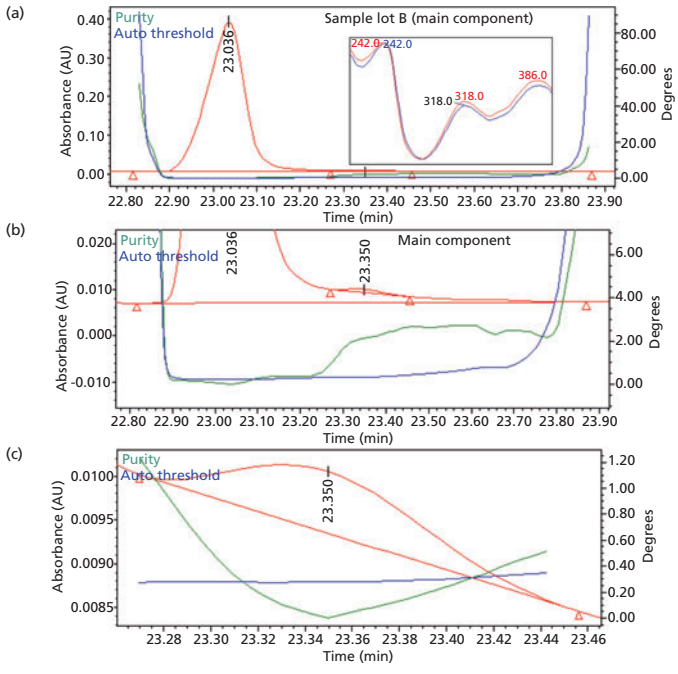

approach. Although the approach has a tremendous upside because of its low cost and relative ease of implementation, great care must be used especially in the interpretation of results from borderline cases where impurities may be present at relatively low levels.

In a subsequent instalment in this series, we will review the principles of advanced curve resolution techniques, and demonstrate how they can be used to provide more robust analyses of peaks composed of both a major and minor component, but still using diode-array spectral data. Finally, we will review the concept of applying 2D-LC separations to the problem of peak purity assessment, which is particularly useful in cases of coeluted compounds that are isomeric or chiral.

Acknowledgement

We thank Dr. Frank Wolf of Agilent Technologies for many helpful discussions during the preparation of this article.

References

(1) International Conference on Harmonization, *Impurities in New Drug Substances Q3A(R2)*, (ICH, Geneva, Switzerland, 2006). http://www.ich.org/fileadmin/Public_Web_Site/ICH_Products/Guidelines/Quality/Q3A_R2/Step4/Q3A_R2__Guideline.pdf (accessed 1 December 2017).

(2) International Conference on Harmonization, *Impurities in New Drug Products Q3B(R2)*, (ICH, Geneva, Switzerland, 2006). http://www.ich.org/fileadmin/Public_Web_Site/ICH_Products/Guidelines/Quality/Q3B_R2/Step4/Q3B_R2__Guideline.pdf (accessed 1 December 2017).

(3) International Conference on Harmonization, *Impurities: Guideline for Residual Solvents Q3C(R6)*, (ICH, Geneva, Switzerland, 2016). http://www.ich.org/fileadmin/Public_Web_Site/ICH_Products/Guidelines/Quality/Q3C/Q3C__R6___Step_4.pdf (accessed 1 December 2017).

(4) International Conference on Harmonization, *Guideline Elemental Impurities Q3D*, (ICH, Geneva, Switzerland, 2014). http://www.ich.org/fileadmin/Public_Web_Site/ICH_Products/Guidelines/Quality/Q3D/Q3D_Step_4.pdf (accessed 1 December 2017).

(5) International Conference on Harmonization, *Pharmaceutical Development Q8(R2)*, (ICH, Geneva, Switzerland, 2009). http://www.ich.org/fileadmin/Public_Web_Site/ICH_Products/Guidelines/Quality/Q8_R1/Step4/Q8_R2_Guideline.pdf (accessed 1 December 2017).

(6) N. Chhabra, M. Aseri, and D. Padmanabhan, *Int. J. Appl. Basic Med. Res.* **3**, 16 (2013). doi:10.4103/2229-516X.112233.

(7) S.K. Teo, W.A. Colburn, W.G. Tracewell, K.A. Kook, D.I. Stirling, M.S. Jaworsky, M.A. Scheffler, S.D. Thomas, and O.L. Laskin, *Clin. Pharmacokinet.* **43**, 311–327 (2004). doi:10.2165/00003088-200443050-00004.

(8) H.-J. Sievert and A. Drouen in: *Diode Array Detection in HPLC*, L. Huber and S.A. George, Eds. (M. Dekker, New York, USA, 1993), pp. 51–126.

(9) M. Stahl, "Peak Purity Analysis in HPLC and CE Using Diode-Array Technology," (2003). https://www.agilent.com/cs/library/applications/5988-8647EN.pdf (accessed 1 December 2017).

(10) "OpenLAB CDS - ChemStation Edition - Understanding Your Spectra Module," (2017). https://www.agilent.com/cs/library/usermanuals/public/CS_LC3D-SpectraModule_A.01.xx_EN.pdf (accessed 1 December 2017).

(11) G. Malikin, "Assessing HPLC Peak Purity with Shimadzu Photodiode Detector SPD-M10Avp," (n.d.). http://www.ssi.shimadzu.com/products/literature/lc/ssiaplc0213.pdf (accessed 1 December 2017).

(12) "Empower PDA Software - Getting Started Guide," (n.d.). http://www.waters.com/webassets/cms/support/docs/71500031503ra.pdf (accessed 1 December 2017).

(13) C.J. Venkatramani, S.R. Huang, M. Al-Sayah, I. Patel, and L. Wigman, *J. Chromatogr. A* **1521**, 63–72 (2017). doi: 10.1016/j.chroma.2017.09.022.

Dwight Stoll is the editor of "LC Troubleshooting". Stoll is an associate professor and co-chair of chemistry at Gustavus Adolphus College in St. Peter, Minnesota, USA. His primary research focus is on the development of 2D-LC for both targeted and untargeted analyses. He has authored or coauthored more than 50 peer-reviewed publications and three book chapters in separation science and more than 100 conference presentations. He is also a member of *LCGC*'s editorial advisory board. Direct correspondence to: LCGCedit@ubm.com

Sarah C. Rutan is a professor of chemistry at Virginia Commonwealth University (VCU), in Richmond, Virginia, USA, where she has been on the faculty for 33 years. Her research spans a broad range of areas in analytical chemistry and chemometrics, and is currently focused on the development of chemometric methods for improving chromatographic analyses, especially comprehensive 2D chromatography. She has more than 100 publications and numerous presentations on these topics.

CJ. Venkatramani is a senior scientist at Genentech USA and has more than 15 years experience in the pharmaceutical industry. He was the key member of the Genentech technical team instrumental in the successful launch of gRed's first small molecule Erivedge, leading from development to commercial launch. His areas of interest include multidimensional chromatography and ultra-trace analysis of genotoxic impurities.

The Column

***LCGC's* global digital magazine** provides unique and timely applications, news, and interviews especially relevant to separation scientists across industry sectors.

SIGN UP FOR **FREE** AT

chromatographyonline.com/column-subscribe

A Compendium of GC Detection, Past and Present

John V. Hinshaw, GC Connections Editor

Gas chromatography makes use of a wide variety of detection methods. In addition to the most often used flame-ionization detection (FID), electron-capture detection (ECD), thermal conductivity detection (TCD), and mass-selective detection (MSD), the list of other detection methods is long. They really shine when deployed properly, but their properties and applications can be a bewildering alphabet soup. This instalment presents a compendium of gas chromatography (GC) detection methods, both past and vanished as well as those that are current and relevant to today's separation challenges.

In the six and a half decades since its inception, gas chromatography (GC) has seen a wide variety of detection methods. Four of them arguably account for greater than 90% of applications today (1): flame-ionization detection (FID), thermal conductivity detection (TCD), electron-capture detection (ECD), and mass-selective detection (MSD). Many more detectors are found in modern chromatography laboratories in smaller quantities, and a few have found their way into the dusty closet of retirement. Ranging from FID to electroantennographic detection (EAD), which uses insect antennae as the sensing elements, GC detection methods cover a wide range of sensitivity and selectivity that is unsurpassed by any other separation method. In 2015, McNair and Schug, writing in "GC Connections" (2), addressed the history and capabilities of eight major GC detection methods, ranging from TCD to the newest member: vacuum ultraviolet (VUV) detection. Along with these mainstream detection methods, the sheer number that are in active use or have been in the past is remarkable—nearly 30 are listed here in Tables 1 and 2. This is not a comprehensive list. Some chromatographers have chosen to use other names and abbreviations, and certainly other varieties may be found that are not as visible to literature searches.

Detector Taxonomy

The International Union of Pure and Applied Chemistry (IUPAC) recently published updated recommendations regarding separation science terminology (3). The publication defines three general types of chromatographic detector. A *universal detector*, such as the thermal conductivity detector, responds to any compound in the column effluent that is different than the carrier gas. A *specific detector* responds only to certain chemically related materials. The electron-capture detector with halogenated compounds, or the aptly named nitrogen–phosphorus detector with nitrogen or phosphorus compounds, are both specific detectors. *Selective detectors* respond to groups of compounds that possess a common measurable characteristic such as mass or spectral absorbance. MSD falls into this group along with VUV and infrared detection (IRD or GC–IR).

The boundaries between these classification are not always clearly defined. Flame photometric detection (FPD), for example, responds to selected spectral emission lines of eluted compounds, and might be considered a selective detection method, but the spectral lines are emitted only by molecules containing certain elements, and thus FPD also is a specific detection method. In a practical sense, FPD is used for its element-specific characteristics, not its spectrally selective nature, so it is best considered a specific detection method. The same logic can be applied to other detection methods.

There is no standard for naming chromatographic detection methods. GC detection method names most often reflect modes of selectivity and specificity. FID, photoionization detection (PID), and many others are generally named after their operating principles. NPD, named for its element specificity, has an alias that refers to its physics: thermionic specific detection (TSD). The latter name is broader and encompasses other operating modes of thermionic detection that are sensitive to other heteroatoms.

Scientists have a love–hate affair with acronyms and abbreviations. They are convenient, short, and easy to misuse. Gas chromatographers have their own unique set that fortunately are related almost one-to-one with GC devices, detectors, inlets, columns, and so-on. For the new (gas) chromatographer the sheer number of terms is bewildering. Perhaps this list can be of assistance navigating the detector bazaar.

Gas chromatography continues to evolve. Every year new GC-related devices appear in publications and in the marketplace. Three new GC detectors have appeared in recent years—vacuum ultraviolet and barrier ionization detectors, and a postcolumn reaction detector. The bulk of GC detectors continues to

Conserve bench space while providing on-demand hydrogen to 1000 mL/min and zero air to 5 lpm

VICI DBS FID Tower Hydrogen + Air Generator

Continuous GC gas supply
(no helium, hydrogen and zero air cylinders) Deionized water is automatically loaded from smart internal system tanks with a 3 liter capacity, providing up to 3000 liters of H2 before a refill is required.

Improves workplace safety and lab efficiency
Ultra high purity carrier grade gas with convenient software control and safety alarm capability. It gives the GC user the option for on-demand hydrogen gas while managing safety concerns. Flow rate from 100 to 1000 mL/min

Increases GC performance and sensitivity
Electrolytic dissociation separates the water into its two main components: hydrogen ready for analytical use, and oxygen that is released into the air.

Ultra high gas purity without the use of dessicants, caustics or palladium
No acid or alkaline solutions are used in the hydrogen generation cycle and the patented automatic drying system ensures the maximum grade of hydrogen purity.

VICI DBS™

sales@vicidbs.com • www.vicidbs.com • +41 (41) 925 62 00

Table 1: GC detection methods

Detection Method	Abbreviation	Description
Atomic emission detection	AED	Atomic emission detection excites eluted compounds in a helium microwave-induced plasma. The resulting atomic emission is detected with an optical spectrometer in the 160–800 nm range. AED is element-specific by observing selected emission lines, much like FPD but with simultaneous multiple emission monitoring. It has sensitivity on par with FID.
Barrier ionization detection	BID	BID uses near-UV light from a dielectric-barrier discharge plasma to ionize eluted compounds. It has sensitivity similar to FID while exhibiting near-universal response.
Electron-capture detection	ECD	An electron-capture detector ionizes solutes by collision with metastable carrier-gas molecules produced by β-emission from a radioactive source such as ^{63}Ni. ECD is one of the most sensitive detection methods, and responds strongly to halogenated solutes and others with a high electron-capture cross-section.
Flame-ionization detection	FID	A flame-ionization detector ionizes hydrocarbon solutes in a hydrogen–air flame. The resulting electrons are collected and measured with a sensitive electrometer. FID is a nearly universal detection method that responds strongly to most classes of organic compounds. Little to no response occurs for CO, CO_2, water, and other compounds that lack C-H bonds.
Flame-photometric detection	FPD	The flame-photometric detector burns eluted solutes in a hydrogen–air flame. The resulting atomic emission lines for sulphur, tin, or phosphorus are selected with an optical interference filter and detected with a photomultiplier. Different optical filters are substituted to observe the emission lines of each specific element.
(Hall) Electrolytic-conductivity detection	HECD, ElCD	In its reductive mode, the electrolytic-conductivity detector catalytically reacts halogen-containing solutes with hydrogen to produce strong acid by-products that are dissolved in a working fluid. The acids dissociate, and the increased electrolytic conductivity of the solution is measured. Other operating modes modify the chemistry for response to nitrogen- or sulphur-containing substances.
Helium ionization detection, discharge ionization detection	HeID, HID, DID	The helium ionization detector operates by creating a helium plasma using radio-frequency excitation; the plasma emits energetic photons that ionize eluted compounds. Additional electrons and metastable helium atoms may also contribute to the response. Earlier versions of these detectors used a radioactive beta particle source similar to ECD. See also PDD.
Infrared detection	IRD or GC–IR	A GC–IR detector obtains mid-infrared spectra of eluted solutes either by direct absorption in a light pipe for gas-phase transmission spectra, or by cryogenic solute trapping on a rotating gold-plated drum or Zn-Se disk for solid-state spectra. IRD distinguishes and identifies eluants by their spectra and by library search. Some peak deconvolution is possible but good peak resolution is preferable.
Mass-selective detection, mass-spectral detection	MSD	MSD provides searchable mass spectra of chromatographic peaks. A variety of mass analyzers have been used, including quadrupole, electric and magnetic sector, ion trap, and time of flight (TOF). Various characteristic mass-fragmentation patterns are provided by sources such as electron ionization (EI) and chemical ionization (CI), both positive and negative (NCI). Total ion current (TIC) chromatograms resemble those from other ionization detectors like the flame-ionization detector. Single-ion monitoring (SIM) and multiple-ion monitoring (MIM) measure selected ions to deduce structural information or to deconvolve coeluted peaks. A second mass analyzer can be added for tandem GC–MS/MS, which engenders further differentiation via selected-reaction monitoring (SRM) and multiple-reaction monitoring (MRM).
Nitrogen–phosphorus detection, thermionic specific detection, thermionic ionization detection	NPD, TSD, TID	NPD catalytically ionizes N- or P-containing solutes on a heated rubidium or cesium surface in a reductive atmosphere. NPD is highly specific with sensitivity somewhat better than FID. Other modes of operation give selectivity for a variety of other heteroatoms.
Photoionization detection	PID	The photoionization detector ionizes solute molecules with photons in the ultraviolet (UV) energy range from a discharge lamp. PID is a specific detection method that responds to aromatics and olefins when operated in the 10.2 eV range, and can respond to other materials with a more energetic light source.
Postcolumn reactors	PCR	Postcolumn reactors convert eluted compounds to others that have different detection characteristics. The most familiar postcolumn device is a nickel-based reducing catalytic converter that produces methane from CO and CO_2, commonly known as a methanizer. The device makes sensitive detection of these compounds possible with a FID. A recent development, the Polyarc reactor (Activated Research Company) converts all carbon-containing peaks to methane in a two-step process of oxidation to CO_2 followed by reduction to CH_4.

Table 1: (continued) GC detection methods

Detection Method	Abbreviation	Description
Pulsed discharge detection	PDD	In its helium ionization mode, PDD uses a pulsed, high-voltage direct current ionization source and helium gas to create photons that ionize eluted peaks. The resulting electrons are collected across biased electrodes. In this mode, PDD is a universal detection method with sensitivity in the low parts-per-billion (ppb, 10^{-9}) range. The addition of a noble gas (Ar, Xe, Kr) can produce specific responses to aromatics and other chemical species. PDD also can be operated in a halogen-specific electron-capture mode, similar to ECD.
Sulphur chemiluminescence detection	SCD	A specific detection method that responds to sulphur-containing compounds by generating and measuring light from chemiluminescence. Compounds are combusted at high temperature to form SO, which then reacts with ozone to produce chemiluminescent emission in the 300–400 nm range.
Thermal-conductivity detection, also katharometer	TCD	TCD measures the differential thermal conductivity of column effluent with reference to pure carrier gas. TCD is a universal detection method with moderate sensitivity. Katharometer is an older name that refers to the use of heated filaments to respond to changes in thermal conductivity. Some thermal conductivity detectors make use of thermistor beads for this function.
Vacuum ultraviolet detection	VUV	The vacuum ultraviolet detector measures the near-UV absorption spectrum of eluted compounds at wavelengths from 115 to 240 nm. It responds to compounds that FID does not, such as CO, O_2, and water, while yielding unique spectra that can deconvolve difficult-to-separate peaks such as *m*- and *p*-xylene.

Table 2: Less common or obsolete GC detection methods

Detection Method	Abbreviation	Description
Acoustic flame detection	AFD	The acoustic flame detector is a unique device built to monitor the oscillation frequency of an unstable flame jet as compounds are eluted through it. AFD also has found application in supercritical fluid chromatography (SFC).
Electroantennographic detection	EAD	Perhaps the most unique GC detection method, EAD has been used to identify the pheromones of moths, bees, beetles, and other insects (5). A single insect antenna or single sensilla is attached to electrodes and exposed to humidified column effluent. Elution of an active compound results in a neuroelectrical response. Compound identification can then be performed with MSD or other selective detection methods.
Gas density balance	GDB	The gas density balance was an early GC detector that used a thermistor-based anemometer to measure differences in the density of pure reference carrier gas and the GC column effluent. It was supplanted by the thermal conductivity detector.
Laser optoacoustic detection	LOD	LOD used the photoacoustic effect with a tunable CO_2 laser to produce limited-range IR spectra of eluted compounds. The sensitivity of LOD was up to 10 times better than FID (4), but it lacked sufficient selectivity to be useful for discrimination of coeluted peaks.
Nuclear magnetic resonance	GC–NMR	A number of researchers have interfaced GC with NMR, either by stopped-flow gas-phase spectral measurement or by semipreparative liquid-phase collection in NMR tubes. Both ^{1}H and ^{13}C NMR spectral data have been used to elucidate ancillary structural information for unknown compounds.
Ultrasonic detection	USD	The ultrasonic detector was an early GC detector that used a pair of acoustical cavities resonant at ultrasonic frequencies to produce a differential beat signal stemming from changes in the velocity of sound in the carrier gas as compounds were eluted. Sensitivity was relatively poor.

see significant application, while only a few have really fallen away into disuse.

References

(1) Author's estimate, not based on published data.

(2) H.M. McNair and K.A. Schug, *LCGC North Am.* **33**(1), 24–33 (2015).

(3) T.A. Maryutina, E.Y. Savonina, P.S. Fedotov, R.M. Smith, H. Siren, and D.B. Hibbert, *Pure Appl. Chem.* **90**(1), 181–231 (2018).

(4) L.B. Kreuzer, *Anal. Chem.* **50**(6), 597A–606A (1978).

(5) J.A. Byers, *J. Neurosci. Methods* **135**, 89–93 (2004).

"GC Connections" editor **John V. Hinshaw** is a senior scientist at Serveron Corporation in Beaverton, Oregon, USA, and a member of *LCGC Asia Pacific*'s editorial advisory board. Direct correspondence about this column to the author via e-mail: LCGCedit@ubm.com

Purification columns

Centrifugal partition chromatography columns offer high-injection capacities of milligrams to multi-kilograms in the natural product purification process, resulting in 95% recoveries with 99% purity.
www.gilson.com/en/AI/Products/80.320/Default.aspx#.Wh19sVWnFaQ
Gilson, Middleton, Wisconsin, USA.

Solid-phase extraction

The hydrophilic-lipophilic balanced polymeric SPE adsorbent Chromabond HLB is specially designed for the enrichment of hydrophilic analytes, including pesticides and pharmaceuticals, from polar matrices such as water, blood serum, or food. Linked hydrophilic groups of the HLB copolymer interact with polar functional groups of the analytes while the lipophilic backbone interacts with nonpolar hydrocarbon residues to provide enhanced retention. Macherey-Nagel offers a broad range of columns, cartridges, and 96-well plates packed with Chromabond HLB adsorbent.
www.mn-net.com
Macherey-Nagel GmbH & Co. KG, Düren, Germany.

Degasser

Biotech's latest Degasi Plus is a further development of Degasi Classic, Degasi GPC, Degasi Micro, and Degasi Semi-Prep. This system can be equipped for various applications. According to the company, the benefits include:
- Smaller footprint
- Weight 1.5 kg (6-channel)
- New vacuum pump using a smart board
- Very quiet
- 1–6 channels
- Parallel connected vacuum chambers
- Ease of troubleshooting and part replacement
- Short lead-time

www.biotech.se
Biotech AB, Onsala, Sweden.

FID gas station

VICI's DBS range of FID gas stations with software control and alarm capability allows GC users to reap the benefits offered by hydrogen carrier gas, whilst overcoming the safety concerns, according to the company. The company reports that this system combines the reliability of the VICI DBS hydrogen and zero air generators into one compact and convenient FID package.
www.VICIDBS.com
VICI AG International, Schenkon, Switzerland.

MALS detector

The new Postnova PN3621 Maximum Angle MALS detector sets a high standard for precise multi-angle light scattering detection for size-exclusion chromatography (SEC) and field-flow fractionation (FFF), according to the company. The detector simultaneously measures the scattering intensity at a maximum of 21 angles, which enables determination of absolute molecular weight and size of proteins, polymers, and nanoparticles.
www.postnova.com
Postnova Analytics GmbH, Landsberg, Germany.

Preparative system

Quattro countercurrent and centrifugal partition chromatographs and extractors are designed to work with, and complement, standard flash and HPLC laboratory and process instrumentation. When appropriate, replacing the solid–liquid columns with unique liquid–liquid instrumentation allows preparations from milligram to tonnes every year. No on-column adsorption or degradation will occur, according to the company. A mass-balance is the norm for CCC/CPC. Typically a 50–80% solvent saving occurs. Standard biphasic solvents, ionic liquids, liquid chiral selectors, and ion exchangers may all be used. According to the company, crude material that would poison standard columns can be injected without causing contamination.
www.quattroprep.com
AECS-QuikPrep Ltd., London, UK.

Microchip column

µPAC is PharmaFluidics' chip-based chromatography column for nano-liquid chromatography. Perfect order in the separation bed is achieved by etching a regular pattern of pillars into a silicon wafer using micromachining technology. The column allows high-resolution separation of tiny, complex biological samples, with an unprecedented robustness. µPAC is suitable for lipidomic, metabolomic, and peptide profiling, according to the company.

www.pharmafluidics.com
PharmaFluidics, Ghent, Belgium.

MALS detector

The µDAWN is, according to the company, the world's first multi-angle light scattering (MALS) detector that can be coupled to any UHPLC system to determine absolute molecular weights and sizes of polymers, peptides, and proteins or other biopolymers directly, without resorting to column calibration or reference standards. The WyattQELS Dynamic Light Scattering (DLS) module, which measures hydrodynamic radii "on-the-fly", reportedly expands the versatility of the µDAWN.

www.wyatt.com
Wyatt Technology, Santa Barbara, California, USA.

Thermal desorption tubes

Designed for material emissions-, flavour-, and air analysis, the TD 3.5+ processes 3.5" tubes or Gerstel plus tubes and offers enhanced recovery and sensitivity, according to the company. The liner-in-liner design without transfer line reduces analyte loss and memory effects. Up to 240 samples are processed automatically. In combination with DHS 3.5+, dynamic headspace from 10 mL up to 1 L volume is performed.

www.gerstel.com
Gerstel GmbH & Co. KG, Mülheim an de Ruhr, Germany.

Nitrogen generator

Peak Scientific's new Infinity XE 50 Series nitrogen generator system is designed to cater for numerous applications across a typical laboratory. Delivering a variable flow of nitrogen gas ranging from 11 L/min to 432 L/min at purities up to 99.5%, the system is ideally suited for a wide range of applications including LC–MS, ELSD, sample evaporation, NMR, FTMS, and gloveboxes.

www.peakscientific.com/infinityxe50
Peak Scientific Instruments Ltd, Glasgow, Scotland, UK.

PDA detector

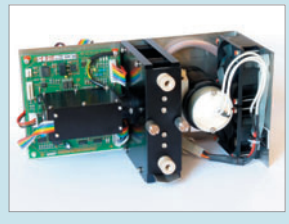

Ecom has developed a mini-PDA monochromator; assembled in an OEM built-in detector with dimensions 220 × 120 × 110 mm (8.66" × 4.72" × 4.33"). The instrument is produced in three versions with wavelength ranges 200–400 nm, 200–600 nm, and 200–800 nm as two-channel, four-channel, or four-channel with scan. A wide assortment of flowcells are available.

www.ecomsro.com
Ecom spol. s r.o., Prague, Czech Republic.

Chromatography software

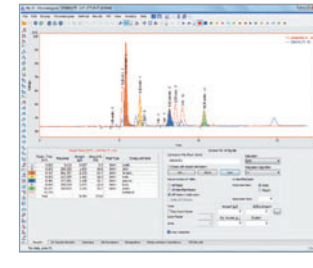

Clarity enables users to control hundreds of different instruments from one environment. The wide range of data acquisition interfaces allows connection to virtually any chromatograph, according to the company. Clarity is multilingual and users can switch between six languages. Clarity reportedly offers easy operation, outstanding user support, and optional extensions for various applications, including PDA, MS, GPC, or NGA. A free demo of the software is available on the company's website.

www.dataapex.com
DataApex, Prague, Czech Republic.

Optimizing SEC for **Biologics Analysis**

An excerpt from *LCGC*'s e-learning tutorial on optimizing size-exclusion chromatography (SEC) for biologics analysis at CHROMacademy.com

Parameters such as pore size, column dimensions, temperature, flow rate, and mobile phase are important to consider when developing robust size-exclusion chromatography (SEC) methods because many of these can impact the level of aggregation detected.

Choosing the optimum pore size for your molecules of interest is very important. You need to ensure the protein monomers and dimers are physically able to permeate the pore structure to obtain a separation. One rule of thumb is that the pore size of the column should be three times the diameter of the molecules of interest. If the pore size is too small, the protein molecules will be excluded from the pores and will be eluted in the void volume of the column, which will result in inaccurate quantitative data. Conversely, if the pore size is too large all of the proteins will be able to fully permeate the particles and there will be very little separation. Because the choice of pore size influences the resolution obtained when using SEC, testing a range of pore sizes to match this to the analytes is worthwhile.

Column internal diameter affects the flow rate and injection volume. There are two common column internal diameters in SEC: 4.6 and 7.8 mm. Since the separation mechanism is purely based on diffusion into and out of the pores of the stationary phase, the greatest separation comes from having larger column sizes. Using a slow flow rate allows the molecules sufficient time to diffuse into and out of the static pool of mobile phase contained within the pore structure. The normal flow rate for a 7.8-mm i.d. SEC column is 1.0 mL/min. This translates to 0.35 mL/min when using a smaller 4.6-mm i.d. column. The internal diameter difference also means the amount of sample injected on a 4.6-mm i.d. column can be reduced by a similar amount (~33%), which is useful if you have a limited amount of sample available. It is important to recognize that operating 4.6-mm i.d. columns at 0.35 mL/min can lead to differences in performance related to the extracolumn dead volume in the system; peaks can become broader if long capillaries with wide bores are used to connect the injection valve to the column or the column to the detector. Longer columns provide more resolution, but require longer run times. Shorter columns produce shorter run times, greatly increasing throughput (for even faster separations, use higher flow rates). Since separation relies on the available pore volume, using longer columns or multiple columns in series increases the available pore volume and therefore increases resolution. Going from a 30-cm column to a 15-cm column means the run time can be cut in half. As long as you still have the required amount of resolution, using a shorter column can greatly improve sample throughput. Sample throughput may be particularly important to you if you are screening multiple samples during early development phases, or taking regular measurements from a fermentation.

Temperature is sometimes overlooked in simple approaches such as the isocratic methods used in SEC. Methods often state the temperature simply as ambient. However, it is highly desirable to use a column oven if you are looking at ensuring good reproducibility. In a laboratory environment where the ambient temperature could change more than 10 °C during the course of the day or night, you will see a noticeable impact. This difference in temperature will change the viscosity of the mobile phase significantly, which in turn will change the column operating pressure, and the diffusion process into and out of the pore structure will also change. The temptation is to increase the temperature—higher temperatures will mean significantly lower viscosity, much lower operating pressures, and much faster diffusion, giving sharper peaks and better resolution. However, if the temperature is too high, more aggregation is likely to result—precipitation of the sample before analysis may even occur because of exposure to excessive temperature.

Chromatographers who work with reversed-phase separations are used to operating at high flow rates and achieving optimum plate counts for small molecules (for example, 1.1–1.2 mL/min on a 300 mm × 7.8 mm column). However, when you start to look at the column efficiency for larger molecules, such as proteins, the optimum flow rate is much lower (in this case, 0.6 mL/min compared to 1.2 mL/min for the previous example). This flow rate difference of course means that the run times will be considerably different.

Mobile-phase selection can have a noticeable effect on some proteins, with differences in ionic strength, pH, and buffer composition resulting in changes in resolution, selectivity, and peak shape. It is therefore essential to consider what effect even minor changes in buffer composition may have to demonstrate method robustness and method optimization. Particular care needs to be taken with detergents and other denaturants because they can cause proteins to unfold and become larger in solution, or can bind to such an extent that molecular weight and size in solution increase dramatically, which leads to shorter retention times. Different columns might behave differently too; most are silica-based and it is common to see undesirable interactions occurring at low ionic strength. However, as you increase ionic strength you may also begin to see other effects; hydrophobic interactions may start to occur as you move towards conditions that begin to look like hydrophobic interaction chromatography.

More Online:
Get the full tutorial at
www.CHROMacademy.com/Essentials
(free until 20 April).

FREE
CHROMACADEMY MEMBERSHIP

Agilent Technologies is offering five years complimentary access to CHROMacademy for all university students and staff.

CHROMacademy is an intuitive, comprehensive e-learning and trouble-shooting platform with more than 3,000 pages of content for HPLC, GC, sample preparation, and hyphenated techniques. No other online resource offers separation scientists more live streaming events, a knowledge base, practical solutions, and new technologies in one easy to navigate website.

Get your free five year membership worth US $1,995* by submitting the form at **www.chromacademy.com/agilent**.

* Five years free access to CHROMacademy only available to customers affiliated with an academic or research institution, conditions apply. A valid university e-mail address if required.

Agilent Technologies

Run, Run, Run!

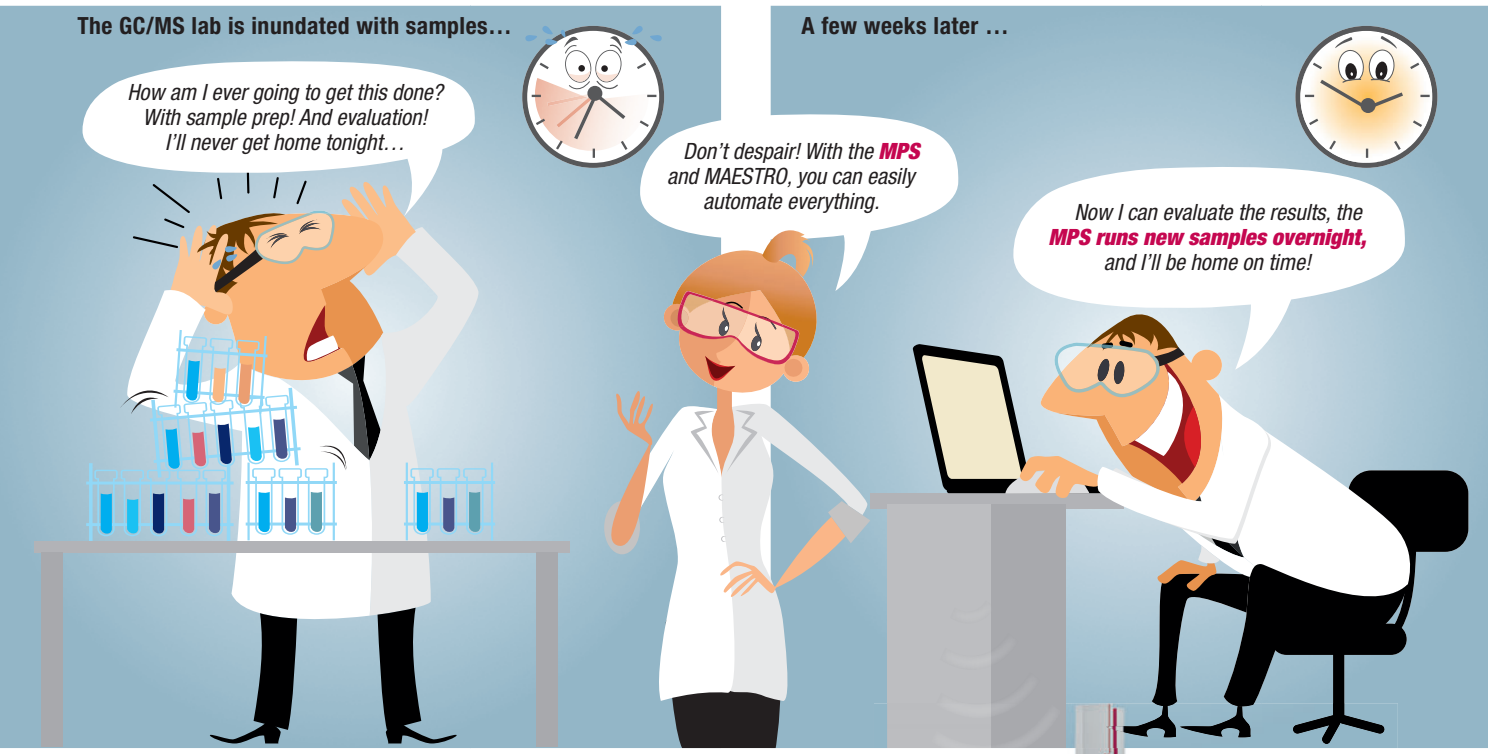

The MultiPurpose Sampler **MPS** automates your sample preparation and introduction for **GC/MS** & **LC/MS** in the easiest possible way.

In the integrated MAESTRO Software, just enter your sample preparation method by mouse-click, step by step.

The daily analysis sequence is set up in no time and automatically checked and verified, making sure that your work gets done on time.

What can we do for you?

Agilent Technologies
Premier Solution Partner

GERSTEL

GERSTEL 50

www.gerstel.com